Plasmas Computed with ATMED CR of the 3rd Non-LTE Code Comparison Workshop Database

In this paper, there are presented some results calculated with ATMED CR of the 3rd Non-LTE Code Comparison Workshop held in December 2003, when this software didn't exist, having been released in 2017. NLTE population kinetics codes were tested of steady-state cases for C, Al, Ar, Ge, Xe and Au plasmas selected for detailed comparisons. The scope of the meeting consisted of analyzing steady-state dense plasma cases of carbon, low temperature plasmas of aluminium and argon, X-ray laser experiments of germanium also with imposing a Planckian radiation field, medium- and high-Z multicharged ions of hot "experiment-related" plasmas of xenon, using real electron temperature and density parameters inferred from electronic and ionic Thomson scattering spectra and finally plasmas of gold. Being motivated by germanium X-ray laser experiments, the time history of electronic temperature T_e and density N_e for a temporal dependent case is provided in Workshop NLTE-3. The calculation with ATMED CR has been carried out to t = 1.975 ns considering the non-uniform time grid along with the corresponding values of T_e and N_e presented, being the initial condition LTE at low temperature.

The results for plasma properties can be considered as relatively precise and optimal, being checked fundamentally the high sensitivity of calculations to changes in regime, local thermodynamic equilibrium (LTE) or non-LTE (NLTE), electronic and radiation temperatures, electronic density and the percentage of hot electrons. Frequency resolved and mean opacities are also displayed computed with ATMED CR using UTA (Unresolved Transition Array) formalism.

Keywords:

Screened Hydrogenic Atomic Model; Collisional Radiative Average Atom Code; Plasmas of NLTE-3 Workshop

1. INTRODUCTION

The collisional radiative model ATMED CR [1,2] constructed in the Average Atom formalism has been developed to calculate plasma population kinetics under coronal, local or non-local thermodynamic equilibrium regimes as an extension of the module named ATMED LTE [3-5] designed previously for local thermodynamic conditions. The atomic model is based on a New Relativistic Screened Hydrogenic Model (NRSHM) with a set of universal screening constants including *nlj*-splitting that has been obtained by fitting to a large database of 61,350 atomic high quality data entries, compiled from the National Institute of Standards and Technology (NIST) database of U.S. Department of Commerce and from the Flexible Atomic Code (FAC) [6,7].

The calculation of accurate relativistic atomic populations including *nlj*-splitting of electronic orbitals, improves the precision of atomic properties as mean charge, rates and the resolution of spectral properties as opacities and radiative power losses, with respect to collisional radiative (CR) average atom codes as XSN of W. Lokke and W. Grasberger of 1977 with *n*-splitting [8,9] or considering *nl*-splitting [10-13]. The CR balance is based on iterative loops for reaching auto convergence in populations and plasma mean charge following the procedure of A.F. Nikiforov et al. [14]. The accuracy ATMED CR code can achieve can be consulted in Section 3 of Ref. [15] which explains in detail the phases of the investigation project, consisting of the comparison of plasma properties of this software with bibliographic data.

The implementation of the collisional radiative balance with the new atomic model, allows now to compute plasmas in NLTE regime or coronal regime, widening considerably for all chemical elements the validity range of thermodynamic conditions [16,17]. In Section 2 there are modeled plasmas with ATMED CR illustrating the high agreement with results for plasma properties of other codes participants of Workshop NLTE-3. Section 3 contains main conclusions. Details about the workshop, motivations for the chosen cases and discussion of some representative results can be found in References [18-19].

2. PLASMAS OF 3RD NLTE DATABASE

The following problems proposed for the cases of C, Al, Ar, Ge, Xe and Au atoms have been calculated with the collisional radiative average atom code ATMED CR. Some graphs are displayed by courtesy of the database (https://nlte.nist.gov/SAHA) for visual comparison of plasma properties. The indicated range of mean charge for NLTE-3 database is approximated. The Radiative Power Losses are indicated in (1e-7 x J)/cm^3/s ≡ erg/cm^3/s.

2.1 Carbon Plasmas

The following problems have been established for the steady-state cases of carbon atoms on a grid of electron temperatures and electron densities, see Table 1 and Figure 1:

Element	Case ID	Total # of Points	Parameter	Grid	# of Points
Carbon	C	7	T_e	10, 15, 20, 30, 45, 60, 80	7
			N_e	10^{22}	1

Table 1. Carbon plasma properties of ATMED CR for comparison with codes of NLTE-3 Workshop

N_e (cm^{-3}) = 10^{22}	ρ (g/cm^3)	Z_{bar} ATMED	Z_{bar} NLTE-3	η_e ATMED CR	RPL (1e-7 J/cm^3/s)
T_e = 10 eV	1.138E-01	1.753E+00	0.5÷2	-2.9307E+00	5.343969E+24
T_e = 15 eV	7.680E-02	2.598E+00	1.25÷2.8	-3.5470E+00	2.052203E+24
T_e = 20 eV	6.250E-02	3.195E+00	1.8÷3.4	-3.9812E+00	1.223476E+24
T_e = 30 eV	5.276E-02	3.781E+00	2.5÷3.8	-4.5934E+00	6.349924E+23
T_e = 45 eV	4.914E-02	4.059E+00	3÷4	-5.2034E+00	3.546953E+23
T_e = 60 eV	4.528E-02	4.404E+00	3.5÷4.5	-5.6356E+00	2.219607E+23
T_e = 80 eV	3.935E-02	5.068E+00	4.4÷5.1	-6.0676E+00	1.348140E+23

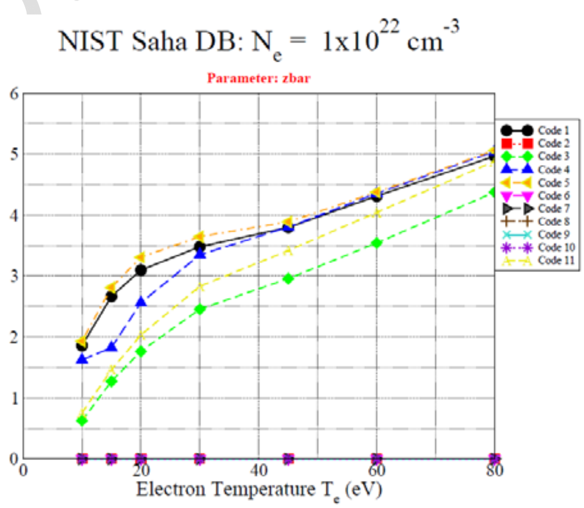

Figure 1.a. Carbon plasma properties computed with codes of NLTE-3 Workshop

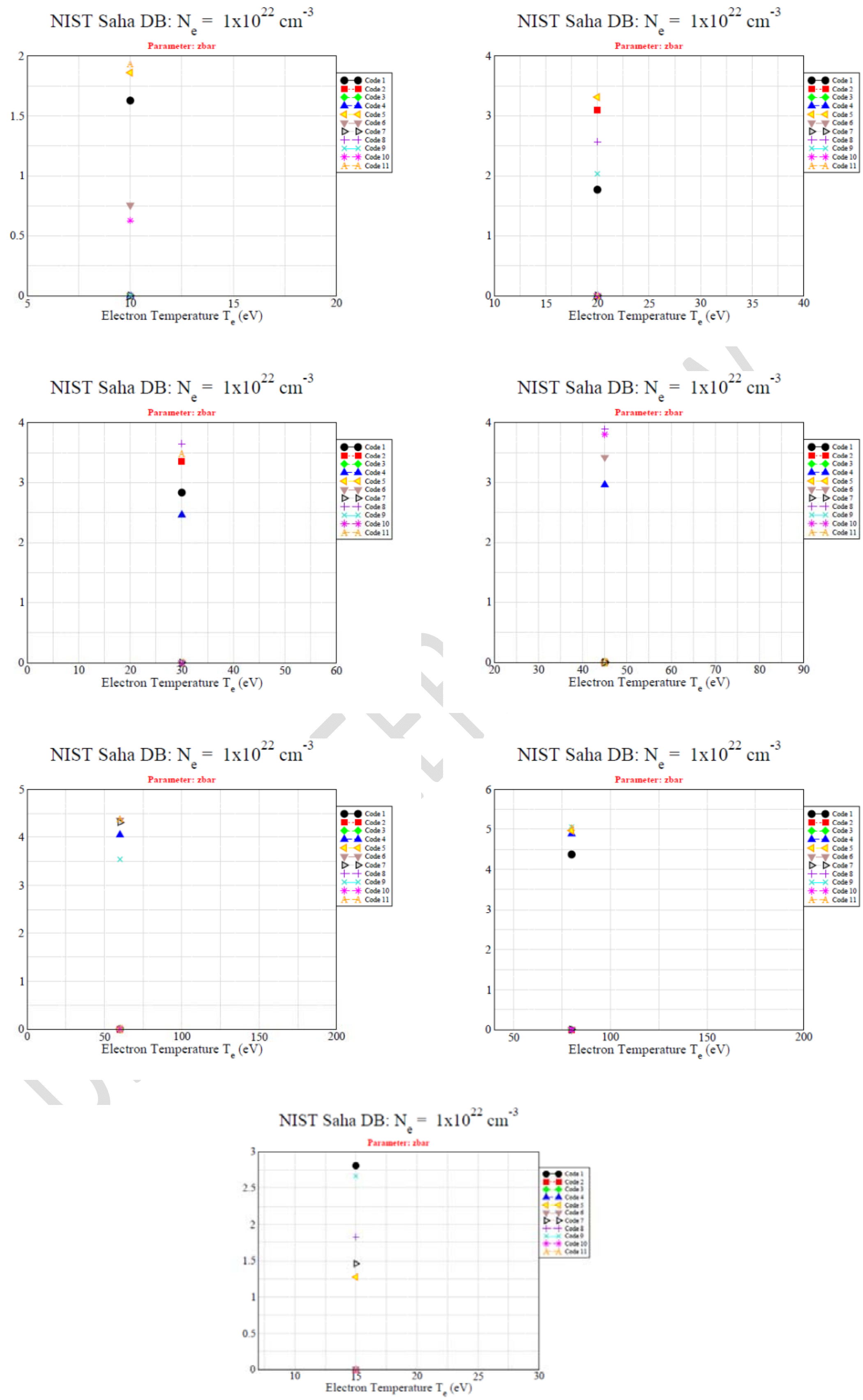

Figure 1.b. Carbon plasma properties computed with codes of NLTE-3 Workshop

2.2 Aluminium Plasmas

The following problems have been established for the steady-state cases of aluminium atoms on a grid of electron temperatures and electron densities, see Table 2 and Figure 2:

Element	Case ID	Total # of Points	Parameter	Grid	# of Points
Aluminum	Al	14	T_e	50, 70, 100, 150, 200, 400, 800	7
			N_e	10^{20}, 10^{22}	2

Table 2. Aluminium plasma properties of ATMED CR for comparison with codes of NLTE-3 Workshop

N_e (cm^{-3}) = 10^{20}	ρ (g/cm^3)	Z_{bar} ATMED	Z_{bar} NLTE-3	η_e ATMED CR	RPL (1e-7 J/cm^3/s)
T_e = 50 eV	5.680E-04	7.933E+00	7.75÷9	-9.9628E+00	3.686132E+18
T_e = 70 eV	5.060E-04	8.866E+00	9.5÷10.5	-1.0472E+01	3.889779E+18
T_e = 100 eV	4.513E-04	9.929E+00	10.5÷11	-1.1008E+01	2.996605E+18
T_e = 150 eV	4.211E-04	1.064E+01	10.5÷11.5	-1.1616E+01	1.683416E+18
T_e = 200 eV	4.131E-04	1.085E+01	10.5÷11.5	-1.2048E+01	1.126856E+18
T_e = 400 eV	4.094E-04	1.094E+01	11÷11.5	-1.3088E+01	1.063361E+18
T_e = 800 eV	4.092E-04	1.095E+01	11÷12.5	-1.4127E+01	2.089232E+18
N_e (cm^{-3}) = 10^{22}	**ρ (g/cm^3)**	**Z_{bar} ATMED**	**Zbar NLTE-3**	**η_e ATMED CR**	**RPL (1e-7 J/cm^3/s)**
T_e = 50 eV	6.357E-02	7.053E+00	5.5÷7.5	-5.3610E+00	4.246858E+23
T_e = 70 eV	5.106E-02	8.781E+00	7.5÷9	-5.8663E+00	2.138201E+23
T_e = 100 eV	4.380E-02	1.023E+01	9.5÷10.5	-6.4022E+00	1.089358E+23
T_e = 150 eV	4.123E-02	1.087E+01	10÷11	-7.0109E+00	6.186111E+22
T_e = 200 eV	4.081E-02	1.098E+01	10.5÷11.5	-7.4426E+00	3.218611E+22
T_e = 400 eV	4.026E-02	1.113E+01	11÷12	-8.4824E+00	4.849790E+22
T_e = 800 eV	3.894E-02	1.151E+01	12.5	-9.5222E+00	6.303487E+22

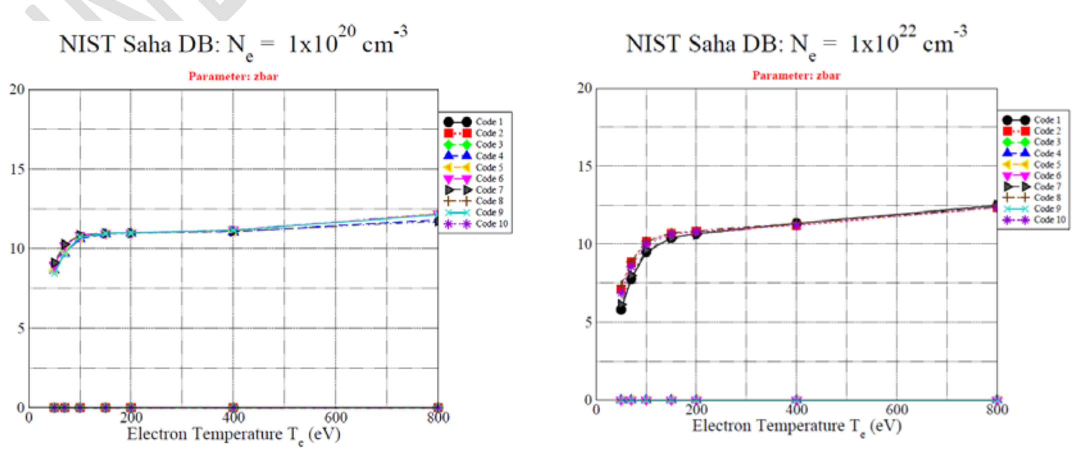

Figure 2.a. Aluminium plasma properties computed with codes of NLTE-3 Workshop

Figure 2.b

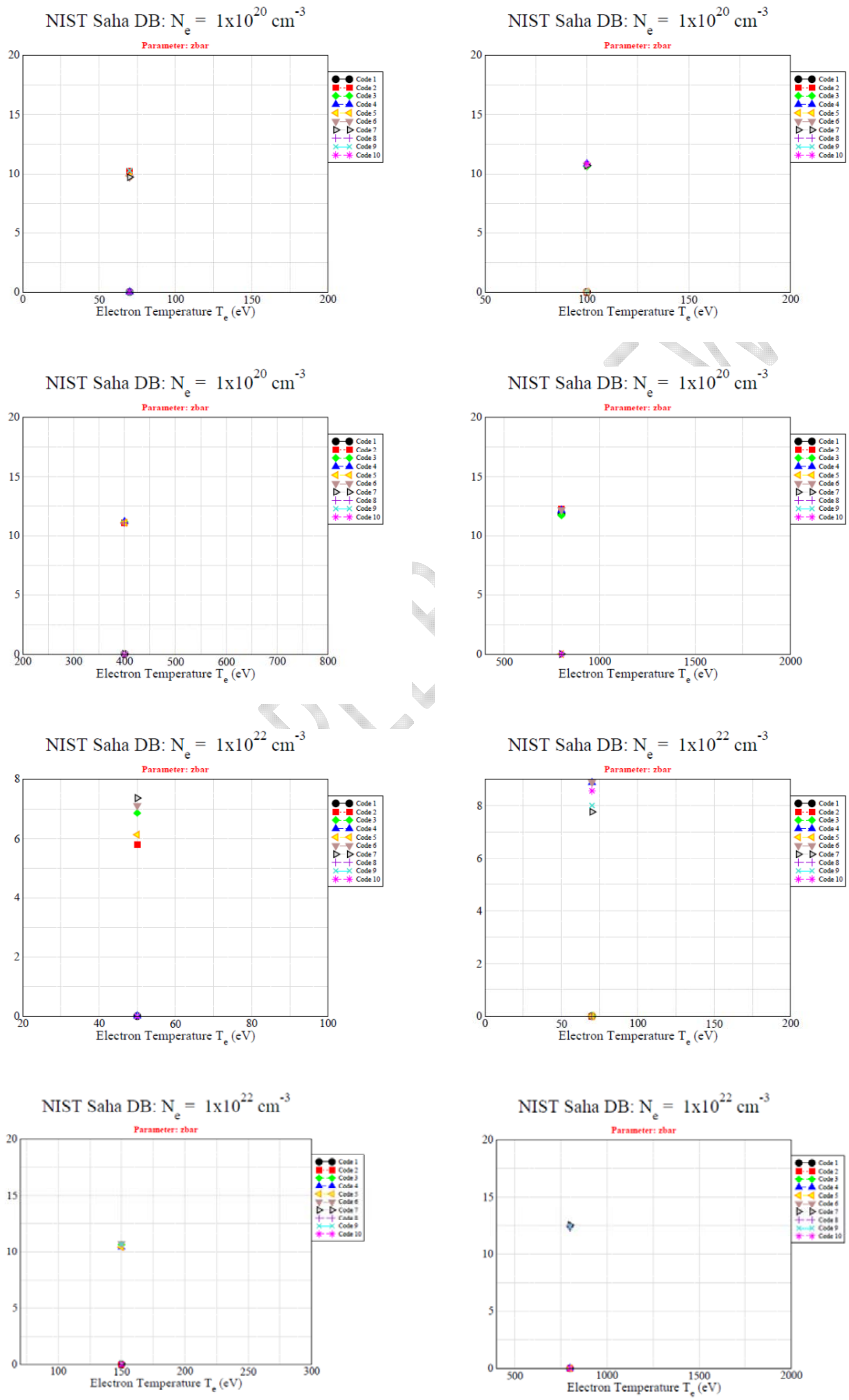

NIST Saha DB: N_e = 1x10^20 cm^-3
Parameter: zbar
Electron Temperature T_e (eV)
NIST Saha DB: N_e = 1x10^22 cm^-3
Code 1
Code 2
Code 3
Code 4
Code 5
Code 6
Code 7
Code 8
Code 9
Code 10

2.3Argon Plasmas

The following problems have been established for the steady-state cases of argon atoms on a grid of electron temperatures and electron densities, see Table 3 and Figure 3:

Element	Case ID	Total # of Points	Parameter	Grid	# of Points
Argon	Ar	24	T_e	100, 300, 600, 1000	4
			N_e	10^{12}, 10^{18}, 10^{23}	3
			T_{hot}	10 000 eV at 0% and 10% of N_e	2

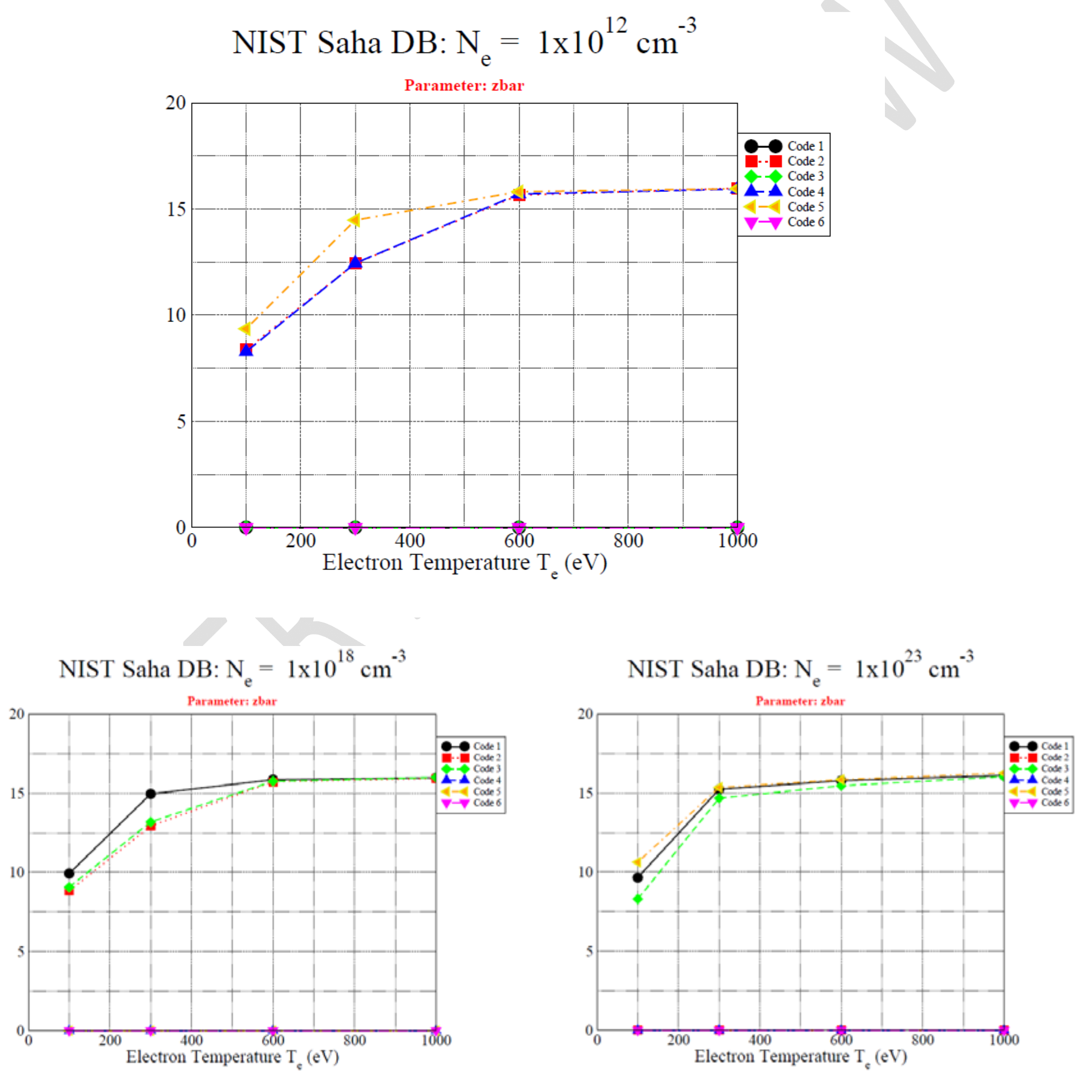

Figure 3.a. Argon plasma properties computed with codes of NLTE-3 Workshop

2.2.1 T_{hot} = 10000 eV at 0% of N_e

It is indicated also the splitting of the bound-free oscillator strength for the case of low density 10^{12} cm^{-3}.

Table 3.a. Argon plasma properties of ATMED CR for comparison with codes of NLTE-3 Workshop

n-splitting & N_e (cm^{-3})=10^{12}	ρ (g/cm^3)	Z_{bar} ATMED	Z_{bar} NLTE-3	η_e ATMED CR	RPL (1e-7 $J/cm^3/s$)
T_e = 100 eV	8.340E-12	8.016E+00	8.5÷10	-2.9421E+01	1.497296E+06
T_e = 300 eV	8.340E-12	8.025E+00	12.5÷15	-3.1068E+01	4.314711E+06
nl-splitting & N_e (cm^{-3})=10^{12}	**ρ (g/cm^3)**	**Z_{bar} ATMED**	**Z_{bar} NLTE-3**	**η_e ATMED CR**	**RPL (1e-7 $J/cm^3/s$)**
T_e = 100 eV	8.340E-12	7.999E+00	8.5÷10	-2.9423E+01	2.445724E+04
T_e = 300 eV	8.300E-12	8.017E+00	12.5÷15	-3.1074E+01	1.170868E+05
N_e (cm^{-3}) = 10^{18}	**ρ (g/cm^3)**	**Z_{bar} ATMED**	**Z_{bar} NLTE-3**	**η_e ATMED CR**	**RPL (1e-7 $J/cm^3/s$)**
T_e = 100 eV	6.948E-06	9.548E+00	8.5÷10	-1.5613E+01	1.240592E+15
T_e = 300 eV	5.616E-06	1.181E+01	12.5÷15	-1.7261E+01	7.847624E+15
T_e = 600 eV	5.500E-06	1.294E+01	15.7÷16	-1.8231E+01	1.973927E+16
T_e = 1000 eV	5.400E-06	1.322E+01	16	-1.8994E+01	3.158257E+16
N_e (cm^{-3}) = 10^{23}	**ρ (g/cm^3)**	**Z_{bar} ATMED**	**Z_{bar} NLTE-3**	**η_e ATMED CR**	**RPL (1e-7 $J/cm^3/s$)**
T_e = 100 eV	1.120E+00	5.927E+00	8÷11	-4.0939E+00	2.499256E+27
T_e = 300 eV	4.580E-01	1.458E+01	14.5÷15.5	-5.7405E+00	8.180175E+25
T_e = 600 eV	4.220E-01	1.577E+01	15÷16	-6.7843E+00	3.201595E+25
T_e = 1000 eV	4.000E-01	1.660E+01	16÷17	-7.5532E+00	2.125694E+25

2.2.2 T_{hot} = 10000 eV at 10% of N_e

Some collisional processes induced by a fraction of 10% very energetic and hot electrons have been also considered at a temperature of T_{hot} = 10 keV, supposing an additive contribution of atomic processes as in Reference of NLTE-4 Workshop [20]. It can be observed that the mean charge is lower for some cases because there are less thermal electrons (90% o a total figure N_e) for promoting bound electrons in excited energy levels up to the continuum. That means, there are 10% hot electrons very energetic producing excitation of electrons in inner shells up to excited energy levels implying a huge jump in energy, but in turn there are 10% less thermal electrons for finally carrying the electrons in excited levels to the continuum.

Table 3.b. Argon plasma properties of ATMED CR of NLTE-3 Workshop

N_e (cm^{-3}) = 10^{23}	Z_{bar} WO hot	Z_{bar} W hot	η_e ATMED CR	ρ W hot (g/cm^3)	ρ WO hot (g/cm^3)
T_e = 100 eV	5.927E+00	4.217E+00	-4.0901E+00	1.580E+00	1.120E+00
T_e = 300 eV	1.458E+01	1.450E+01	-5.7463E+00	4.580E-01	4.580E-01
T_e = 600 eV	1.577E+01	1.573E+01	-6.7868E+00	4.220E-01	4.220E-01
T_e = 1000 eV	1.660E+01	1.651E+01	-7.5464E+00	4.050E-01	4.000E-01

2.3 Germanium Plasmas

The following problems have been established for the steady-state cases of germanium atoms on a grid of electron temperatures and electron densities, see Table 4 and Figure 4:

2.3.1 T_{rad} = 0 eV

Element	Case ID	Total # of Points	Parameter	Grid	# of Points
Germanium	Ge	12	T_e	150, 250, 400, 600	4
			N_e	10^{17}, 10^{20}, 3×10^{22}	3

Table 4.a. Germanium plasma properties of ATMED CR for comparison with codes of NLTE-3 Workshop

N_e (cm^{-3}) = 10^{17}	ρ (g/cm^3)	Z_{bar} ATMED	Z_{bar} NLTE-3	η_e ATMED CR	RPL (1e-7 J/cm^3/s)
T_e = 150 eV	1.050E-06	1.152E+01	12÷17.5	-1.8522E+01	3.554017E+14
T_e = 250 eV	9.400E-07	1.327E+01	15÷20	-1.9257E+01	8.083488E+14
T_e = 400 eV	8.452E-07	1.453E+01	17÷22	-1.9978E+01	1.160658E+15
T_e = 600 eV	5.660E-07	2.182E+01	20÷22	-2.0580E+01	3.582530E+14
N_e (cm^{-3}) = 10^{20}	**ρ (g/cm^3)**	**Z_{bar} ATMED**	**Z_{bar} NLTE-3**	**η_e ATMED CR**	**RPL (1e-7 J/cm^3/s)**
T_e = 150 eV	7.400E-04	1.643E+01	15÷20	-1.1609E+01	7.121588E+19
T_e = 250 eV	6.439E-04	1.874E+01	18÷22	-1.2382E+01	7.559920E+19
T_e = 400 eV	5.922E-04	2.037E+01	20÷22	-1.3088E+01	6.305504E+19
T_e = 600 eV	5.720E-04	2.109E+01	21÷22.5	-1.3696E+01	5.414345E+19
N_e (cm^{-3}) = 3×10^{22}	**ρ (g/cm^3)**	**Z_{bar} ATMED**	**Z_{bar} NLTE-3**	**η_e ATMED CR**	**RPL (1e-7 J/cm^3/s)**
T_e = 150 eV	1.969E-01	1.839E+01	17÷20	-5.9112E+00	4.086265E+24
T_e = 250 eV	1.722E-01	2.102E+01	20÷22	-6.6781E+00	2.217217E+24
T_e = 400 eV	1.665E-01	2.174E+01	21.5÷24	-7.3835E+00	2.667664E+24
T_e = 600 eV	1.610E-01	2.247E+01	23÷26	-7.9921E+00	1.254399E+24

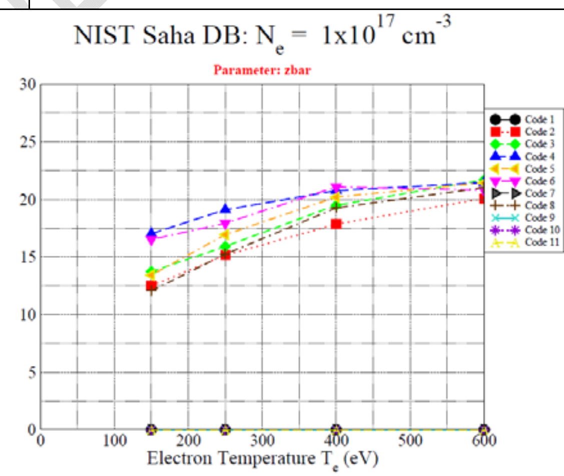

Figure 4.a. Germanium plasma properties computed with codes of NLTE-3 Workshop

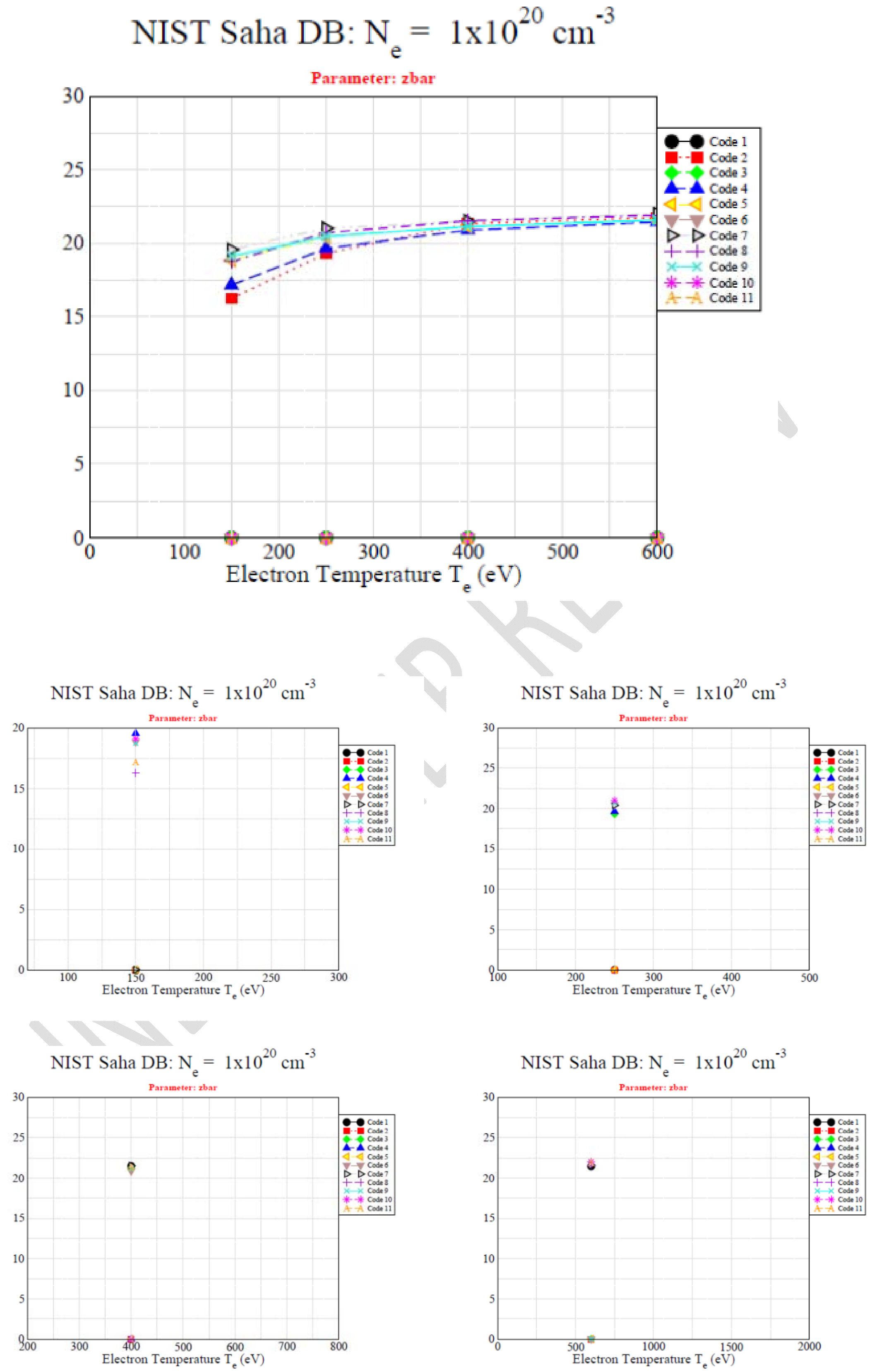

Figure 4.b. Germanium plasma properties computed with codes of NLTE-3 Workshop

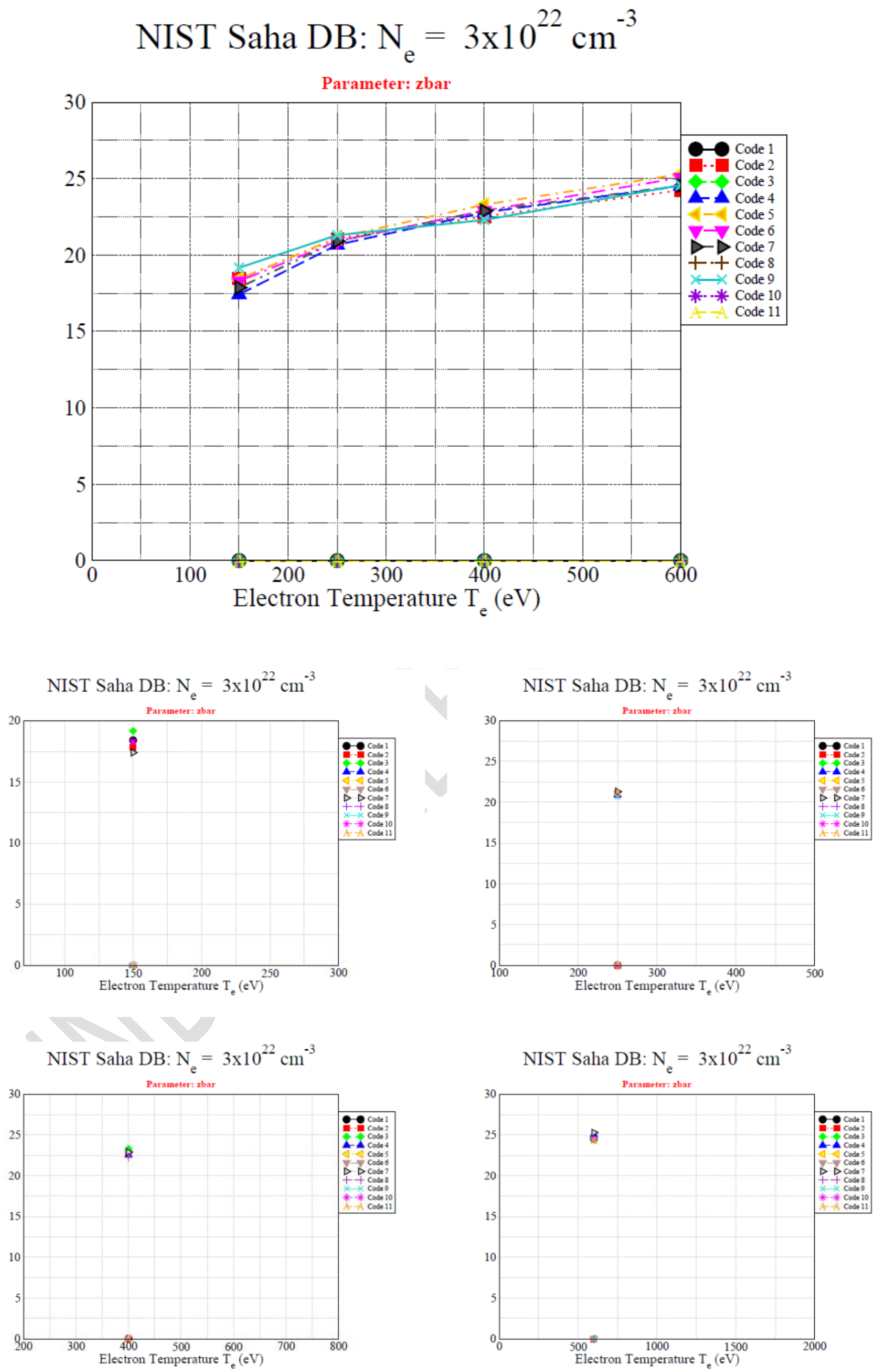

Figure 4.c. Germanium plasma properties computed with codes of NLTE-3 Workshop

2.3.2 $T_{rad} \neq 0$ eV & $N_e = 3x10^{22}$ cm^{-3}

Element	Case ID	Total # of Points	Parameter	Grid	# of Points
Germanium	GeTr	11	T_e	150, 250, 400, 600	4
			N_e	3×10^{22}	1
			T_{rad}	$T_e/2$, T_e, 300	3

Table 4.b. Germanium plasma properties of ATMED CR for comparison with codes of NLTE-3 Workshop at T_{rad} (eV)

T_{rad} = $T_e/2$	Z_{bar} $T_{rad} = 0$	Z_{bar} $T_{rad} \neq 0$	ρ (g/cm^3)	η_e ATMED CR	RPL (1e-7 J/cm^3/s)
T_e = 150 eV	1.839E+01	1.843E+01	1.964E-01	-5.9113E+00	2.351269E+24
T_e = 250 eV	2.102E+01	2.108E+01	1.717E-01	-6.6784E+00	8.856310E+24
T_e = 400 eV	2.174E+01	2.194E+01	1.649E-01	-7.3837E+00	2.078181E+24
T_e = 600 eV	2.247E+01	2.428E+01	1.491E-01	-7.9915E+00	7.307794E+23
T_{rad} = T_e	**Z_{bar} $T_{rad} = 0$**	**Z_{bar} $T_{rad} \neq 0$**	**ρ (g/cm^3)**	**η_e ATMED CR**	**RPL (1e-7 J/cm^3/s)**
T_e = 150 eV	1.839E+01	1.883E+01	1.922E-01	-5.9114E+00	3.787635E+24
T_e = 250 eV	2.102E+01	2.231E+01	1.622E-01	-6.6784E+00	9.433184E+23
T_e = 400 eV	2.174E+01	2.681E+01	1.350E-01	-7.3836E+00	3.880911E+23
T_e = 600 eV	2.247E+01	2.952E+01	1.226E-01	-7.9917E+00	2.607794E+23
T_{rad} = 300	**Z_{bar} $T_{rad} = 0$**	**Z_{bar} $T_{rad} \neq 0$**	**ρ (g/cm^3)**	**η_e ATMED CR**	**RPL (1e-7 J/cm^3/s)**
T_e = 150 eV	1.839E+01	2.179E+01	1.700E-01	-5.8885E+00	1.138688E+24
T_e = 250 eV	2.102E+01	2.383E+01	1.550E-01	-6.6580E+00	4.655749E+23
T_e = 400 eV	2.174E+01	2.381E+01	1.520E-01	-7.3836E+00	6.503707E+23
T_e = 600 eV	2.247E+01	2.428E+01	1.491E-01	-7.9915E+00	7.307794E+23

2.3.3 Frequency Resolved & Mean Opacities

The interaction of radiation with matter is determined by the behaviour of electrons in the electromagnetic field of radiation. Depending on the initial and final states of the electron, the code divides the photon absorption processes in three groups: bound-bound, bound-free and free-free transitions. The code ATMED CR performs a calculation of opacities based on the average atom model, where atomic data, binding energies, oscillator strengths, transition probabilities, etc., are obtained from the relativistic screened hydrogenic model. In the formulas for atomic processes, if transitions are or not allowed is implemented through oscillator strengths.

The use of several cross sections, quantum or reduced, has been tested, considering as a reference the opacity calculated by the code ATMED LTE, where the mean charge and the populations are practically equal to ones computed after solving the CR balance for a plasma in LTE regime. And now the cross sections used are indicated in schematic form, detailing their meaning in the references. There are two absorption cross sections of the radiation field in spectral lines for bound-bound transitions between relativistic orbitals:

- Bound-Bound Absorption Cross Section (Rozsnyai-Nikiforov [12-14]) ~ Mixed UTA:

$$\sigma_{bb}(h\nu) = 2\pi^2 \alpha a_0 e^2 f_{kk'} S_{kk'}(h\nu) \quad (1)$$

- Bound-Bound Absorption Cross Section ([5]) ~ UTA/STA:

$$\sigma_{kk'}^{bb}(h\nu) = \frac{\pi h e^2}{m_e c} \sum_{kk'} P_k \; f_{kk'} S_{kk'}(h\nu) \quad (2)$$

where:

$f_{kk'}$: Photon absorption oscillator strength for the transition from the orbital k to other k' developed in Laguerre polynomials and based on wavefunctions constructed with relativistic screened charges [5-7].

$S_{kk'}(h\nu)$: Voigt profile which includes Doppler, Natural, Stark and Dielectronic broadenings.

The first, Equation (1), provides a discrete structure of lines which retains in the spectrum the lines of high intensity between the relativistic orbitals of the average atom which represents the plasma, being equivalent to apply the formalism MUTA (Mixed Unresolved Transition Array) in the spectrum calculated by a detailed code [9]. The second, Equation (2), is the average of the first one Equation (1), which provides general characteristics of the absorption spectrum being equivalent to apply the formalism UTA (Unresolved Transition Array). It is considered also the dielectronic broadening which implies the statistical grouping of lines computing greater values of Rosseland mean opacity, being very sensitive to the regions of low opacity in the frequency resolved spectrum. The UTA spectral structures are sometimes shifted in photon energy with respect to detailed spectra of DLA/DTA codes as density increases due to more separated lines of the same array of electronic transitions. Depending on the calculated plasma, a greater or lower degree of agreement between UTA and MUTA formalisms is obtained in the order of magnitude of Rosseland (K_R) and Planck (K_P) mean opacities. The greater the density, the better the concordance of figures of K_R. The values of K_P are in good agreement for practically all displayed plasma cases.

The greater the temperature at high density as 3 x 10^{22} cm^{-3}, the bigger the departure between computed with UTA formalism considering T_e = T_{rad} or T_{rad} = 0 eV, see Figures 4d÷4f.

Table 4.c. Germanium plasma mean opacities of ATMED CR UTA or MUTA of NLTE-3 Workshop at T_{rad} (eV)

T_e = 250 eV & N_e = 1E+17 cm^{-3}	**K_R UTA (cm^2/g)**	**K_R MUTA (cm^2/g)**	**K_P UTA (cm^2/g)**	**K_P MUTA (cm^2/g)**
T_{rad} = 0	1.425E+03	1.241E+02	3.797E+03	2.745E+03
T_e = 250 eV & N_e = 1E+20 cm^{-3}	**K_R UTA (cm^2/g)**	**K_R MUTA (cm^2/g)**	**K_P UTA (cm^2/g)**	**K_P MUTA (cm^2/g)**
T_{rad} = 0	8.835E+02	1.049E+02	2.518E+03	2.182E+03
T_e = 400 eV & N_e = 1E+17 cm^{-3}	**K_R UTA (cm^2/g)**	**K_R MUTA (cm^2/g)**	**K_P UTA (cm^2/g)**	**K_P MUTA (cm^2/g)**
T_{rad} = 0	8.425E+02	9.233E+01	2.952E+03	2.174E+03
T_e = 400 eV & N_e = 1E+20 cm^{-3}	**K_R UTA (cm^2/g)**	**K_R MUTA (cm^2/g)**	**K_P UTA (cm^2/g)**	**K_P MUTA (cm^2/g)**
T_{rad} = 0	5.854E+02	7.913E+01	2.321E+03	1.999E+03
T_e = 600 eV & N_e = 1E+17 cm^{-3}	**K_R UTA (cm^2/g)**	**K_R MUTA (cm^2/g)**	**K_P UTA (cm^2/g)**	**K_P MUTA (cm^2/g)**
T_{rad} = 0	1.230E+01	1.415E+00	1.766E+03	1.397E+03
T_e = 600 eV & N_e = 1E+20 cm^{-3}	**K_R UTA (cm^2/g)**	**K_R MUTA (cm^2/g)**	**K_P UTA (cm^2/g)**	**K_P MUTA (cm^2/g)**
T_{rad} = 0	3.527E+02	7.229E+01	1.793E+03	1.490E+03
T_e = 150 eV & N_e = 3E+22 cm^{-3}	**K_R UTA (cm^2/g)**	**K_R MUTA (cm^2/g)**	**K_P UTA (cm^2/g)**	**K_P MUTA (cm^2/g)**
T_{rad} = 0	1.133E+03	6.893E+02	3.349E+03	3.268E+03
T_{rad} = T_e/2	2.288E+03	1.085E+03	6.623E+03	6.130E+03
T_{rad} = 300 eV	3.311E+02	1.378E+02	1.857E+03	1.730E+03
T_{rad} = T_e	9.896E+02	6.147E+02	3.089E+03	3.017E+03
T_e = 250 eV & N_e = 3E+22 cm^{-3}	**K_R UTA (cm^2/g)**	**K_R MUTA (cm^2/g)**	**K_P UTA (cm^2/g)**	**K_P MUTA (cm^2/g)**
T_{rad} = 0	3.625E+02	1.858E+02	1.823E+03	1.700E+03
T_{rad} = T_e/2	3.902E+02	3.013E+02	2.026E+03	1.881E+03
T_{rad} = 300 eV	1.274E+02	5.841E+01	1.341E+03	1.286E+03
T_{rad} = T_e	1.796E+02	9.895E+01	1.428E+03	1.345E+03
T_e = 400 eV & N_e = 3E+22 cm^{-3}	**K_R UTA (cm^2/g)**	**K_R MUTA (cm^2/g)**	**K_P UTA (cm^2/g)**	**K_P MUTA (cm^2/g)**
T_{rad} = 0	3.708E+02	1.246E+02	2.064E+03	1.878E+03
T_{rad} = T_e/2	1.991E+02	1.423E+02	1.229E+03	1.174E+03
T_{rad} = 300 eV	1.421E+02	6.575E+01	1.357E+03	1.308E+03
T_{rad} = T_e	7.595E+01	2.881E+01	8.314E+02	8.195E+02
T_e = 600 eV & N_e = 3E+22 cm^{-3}	**K_R UTA (cm^2/g)**	**K_R MUTA (cm^2/g)**	**K_P UTA (cm^2/g)**	**K_P MUTA (cm^2/g)**
T_{rad} = 0	3.071E+02	1.028E+02	1.580E+03	1.390E+03
T_{rad} =T_e/2=300 eV	1.262E+02	6.030E+01	1.248E+03	1.217E+03
T_{rad} = T_e	1.120E+01	6.740E+00	1.156E+02	1.153E+02

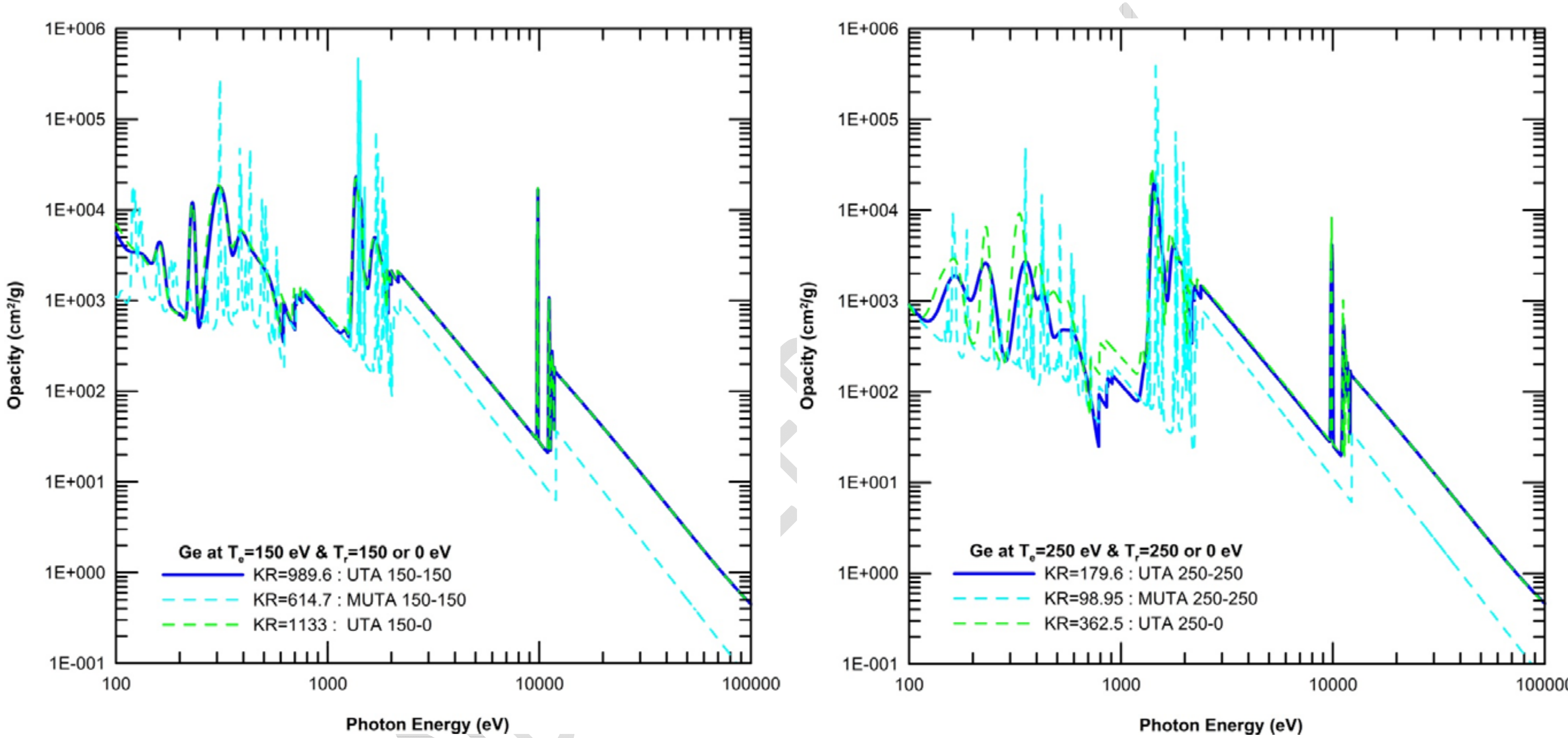

Figure 4.d. Frequency resolved opacity of germanium plasma at density 3E+22 cm^{-3} with ATMED CR at T_{rad} = 150 eV in UTA (—) or MUTA (—) formalisms or T_{rad} = 0 eV in UTA (—) formalism and T_e = 150 eV observing the sensitivity to departures from LTE regime (left). Germanium plasma frequency resolved opacity of ATMED CR at T_{rad} = 250 eV in UTA (—) or MUTA (—) formalisms or T_{rad} = 0 eV in UTA (—) formalism and T_e = 250 eV observing the sensitivity to departures from LTE regime (right).

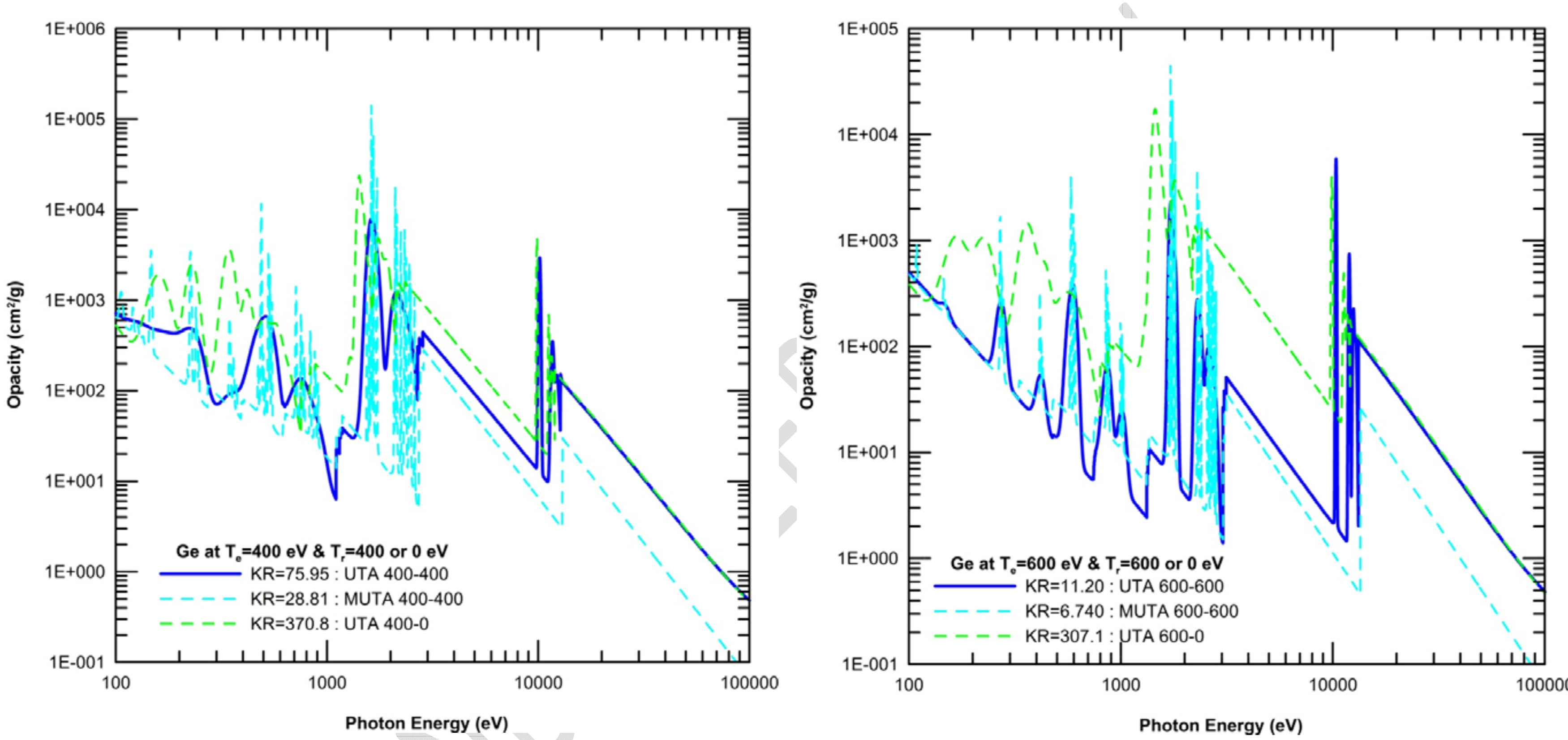

Figure 4.e. Frequency resolved opacity of germanium plasma at density 3E+22 cm^{-3} with ATMED CR at T_{rad} = 400 eV in UTA (—) or MUTA (—) formalisms or T_{rad} = 0 eV in UTA (—) formalism and T_e = 400 eV observing the sensitivity to departures from LTE regime (left). Germanium plasma frequency resolved opacity of ATMED CR at T_{rad} = 600 eV in UTA (—) or MUTA (—) formalisms or T_{rad} = 0 eV in UTA (—) formalism and T_e = 600 eV observing the sensitivity to departures from LTE regime (right).

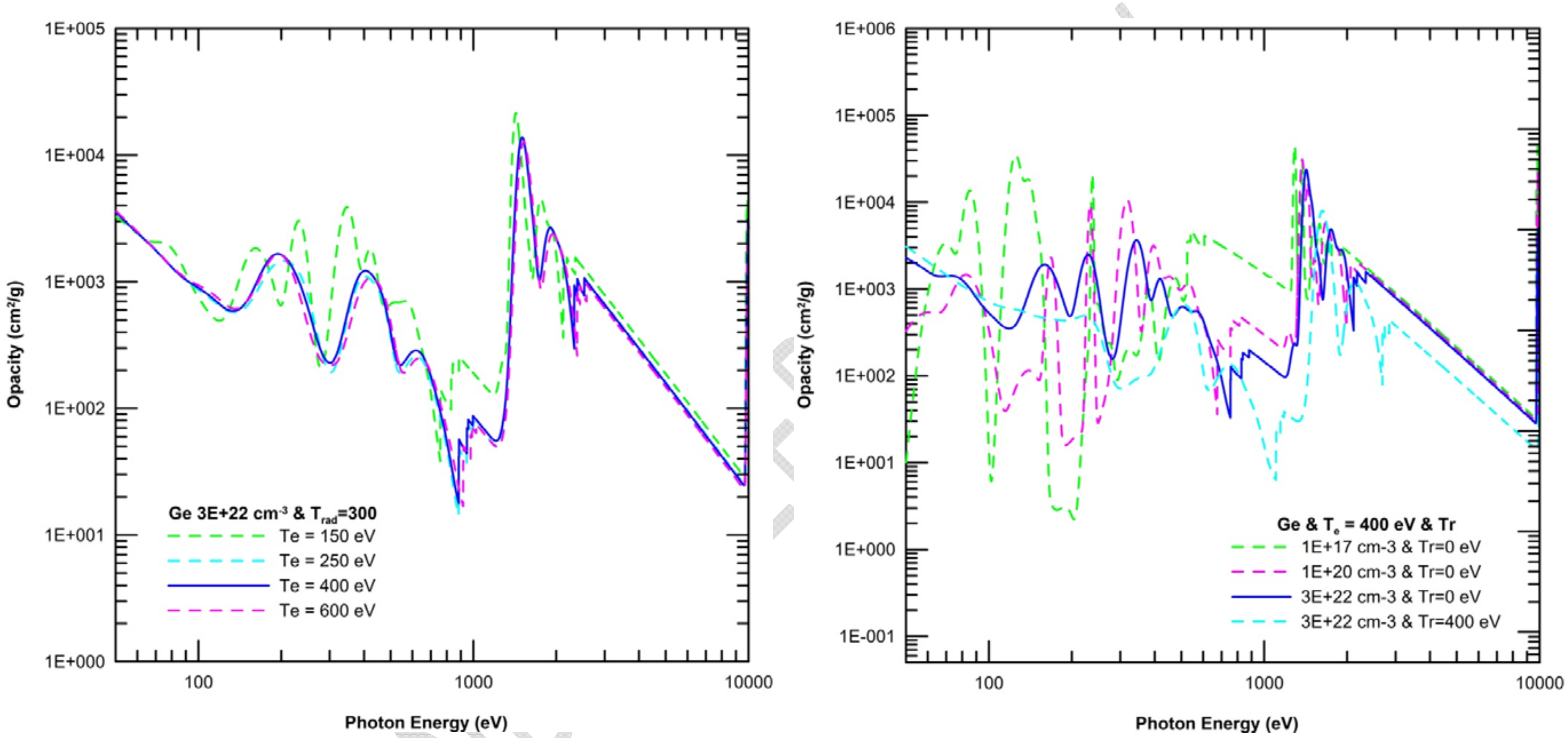

Figure 4.f. Germanium plasma frequency resolved opacity of ATMED CR at T_{rad} = 300 eV and T_e = 150 (—), 250 (—), 400 (—) and 600 (—) eV observing the sensitivity to electronic temperature variation (left). Germanium plasma properties of ATMED CR at T_{rad} = 0 eV, T_e = 400 eV (—) at N_e = 3E+22 cm^{-3}; T_{rad} = T_e = 400 eV (—) at N_e = 3E+22 cm^{-3} and T_e = 400 eV and densities N_e = 1E+17 (—), 1E+20 (—) cm^{-3} observing the sensitivity to density and radiation temperature variations (right).

2.4 Xenon Plasmas

The following problems have been established for the steady-state cases of xenon atoms on a grid of electron temperatures and electron densities, see Table 5 and Figure 5:

Element	Case ID	Total # of Points	Parameter	Grid	# of Points
Xenon	Xe	6	T_e	200, 375, 415, 455, 600, 750	6
			N_i (ion!)	4.75×10^{18}	1
			Spectrum	9−120 Å	2221

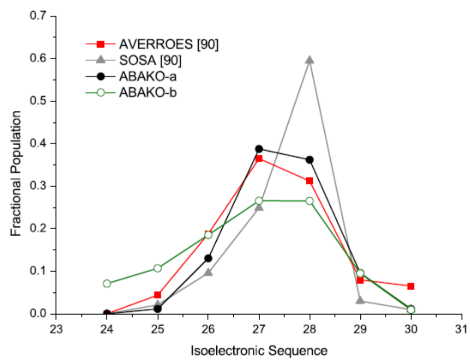

TABLE VII. Average ionization for the Xe plasma created at LULI [96] and calculations obtained by different models. For ABAKO and AVERROES the ion density $n_{ion}=4.75\times10^{18}$ cm^{-3} and T_e=450 eV are input parameters. For the SOSA fit a value of T_e =400 eV was assumed.

Source	$\bar{Z}$
Experiment [96]	27.4 ± 1.5
ABAKO-a	26.6
ABAKO-b	27.1
AVERROES [96]	26.8
SOSA fit [96]	26.5

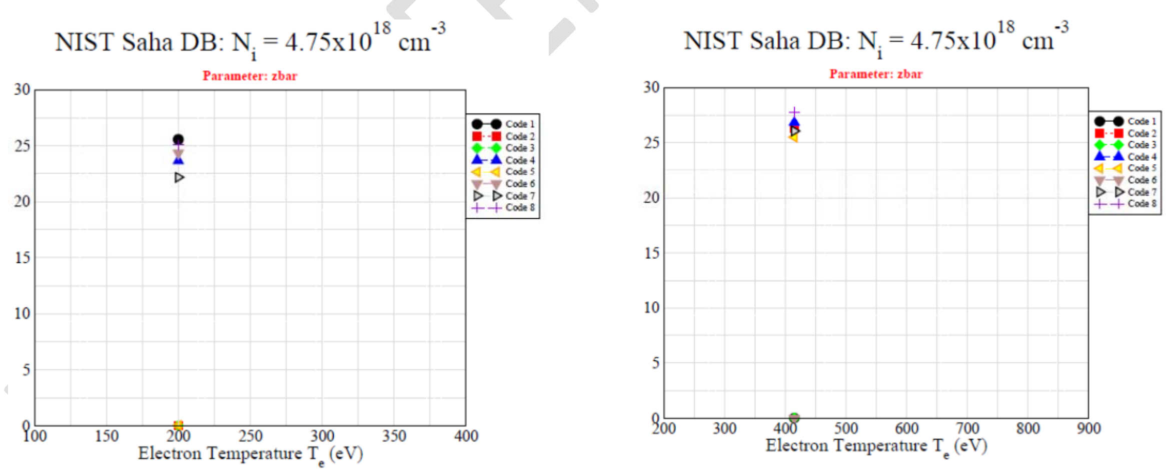

Figure 5.a. Charge state distributions simulated by CR detailed models for xenon experiment carried out in LULI facility [21]. Mean charge of xenon created in LULI facility. Calculations obtained for N_i=4.75x10^{18} cm^{-3} and T_e=450 eV.

It can be observed for xenon plasmas created in LULI facility [21], the appreciable difference in this element plasma properties, especially for mean charge, depending on if it is used the maximum principal quantum number n_{max}= 6 or 10.

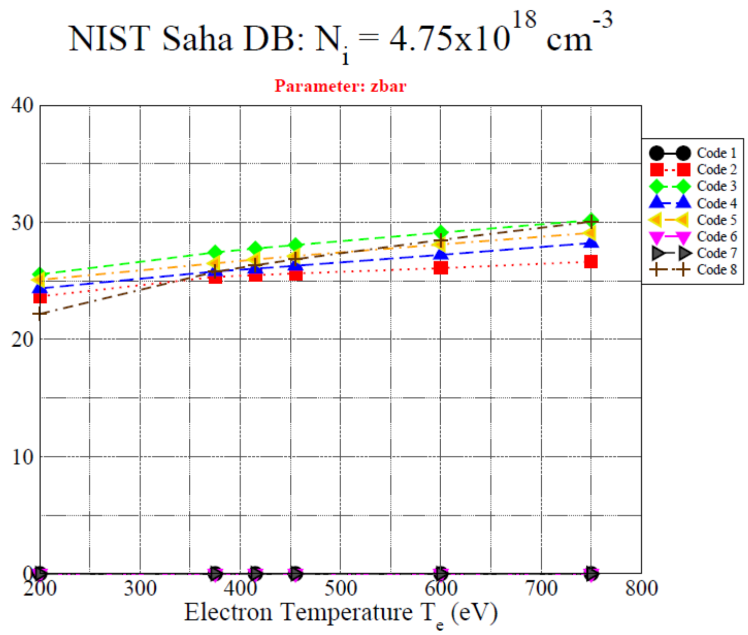

Figure 5.b. Xenon plasma properties computed with codes of NLTE-3 Workshop

Table 5. Xenon plasma properties of ATMED CR for comparison with codes of NLTE-3 Workshop

T_e (eV) = 200	**ρ (g/cm^3)**	**N_e (cm^{-3})**	**N_{ion} (ion.cm^{-3})**	**Z_{bar} NLTE-3**	**Z_{bar} ATMED**	**RPL (J/cm^3/s)**
n_{max} = 6	1.0356E-03	1.162E+20	4.750E+18	22÷25.5	2.447E+01	1.583445E+13
n_{max} = 10	1.0356E-03	1.246E+20	4.750E+18	22÷25.5	2.624E+01	2.991353E+15
T_e (eV) = 375	**ρ (g/cm^3)**	**N_e (cm^{-3})**	**N_{ion} (ion.cm^{-3})**	**Z_{bar} NLTE-3**	**Z_{bar} ATMED**	**RPL (J/cm^3/s)**
n_{max} = 6	1.0356E-03	1.217E+20	4.750E+18	25÷27.5	2.561E+01	1.568357E+13
n_{max} = 10	1.0356E-03	1.406E+20	4.750E+18	25÷27.5	2.959E+01	1.081961E+15
T_e (eV) = 415	**ρ (g/cm^3)**	**N_e (cm^{-3})**	**N_{ion} (ion.cm^{-3})**	**Z_{bar} NLTE-3**	**Z_{bar} ATMED**	**RPL (J/cm^3/s)**
n_{max} = 6	1.0356E-03	1.223E+20	4.750E+18	25÷27.5	2.575E+01	1.510424E+13
n_{max} = 10	1.0356E-03	1.438E+20	4.750E+18	25÷27.5	3.028E+01	7.868060E+15
T_e (eV) = 455	**ρ (g/cm^3)**	**N_e (cm^{-3})**	**N_{ion} (ion.cm^{-3})**	**Z_{bar} NLTE-3**	**Z_{bar} ATMED**	**RPL (J/cm^3/s)**
n_{max} = 6	1.0356E-03	1.229E+20	4.750E+18	25.5÷28	2.587E+01	1.557981E+13
n_{max} = 10	1.0356E-03	1.464E+20	4.750E+18	25.5÷28	3.082E+01	4.913842E+15
T_e (eV) = 600	**ρ (g/cm^3)**	**N_e (cm^{-3})**	**N_{ion} (ion.cm^{-3})**	**Z_{bar} NLTE-3**	**Z_{bar} ATMED**	**RPL (J/cm^3/s)**
n_{max} = 6	1.0356E-03	1.247E+20	4.750E+18	26÷29	2.625E+01	1.830720E+13
n_{max} = 10	1.0356E-03	1.525E+20	4.750E+18	26÷29	3.210E+01	8.147788E+15
T_e (eV) = 750	**ρ (g/cm^3)**	**N_e (cm^{-3})**	**N_{ion} (ion.cm^{-3})**	**Z_{bar} NLTE-3**	**Z_{bar} ATMED**	**RPL (J/cm^3/s)**
n_{max} = 6	1.0356E-03	1.264E+20	4.750E+18	26÷30.5	2.661E+01	1.944406E+13
n_{max} = 10	1.0356E-03	1.578E+20	4.750E+18	26÷30.5	3.322E+01	9.224302E+14

2.5 Gold Plasmas

The following problems have been established for the steady-state cases of gold atoms on a grid of electron temperatures and electron densities. See Table 6 and Figure 6:

Element	Case ID	Total # of Points	Parameter	Grid	# of Points
Gold	Au	18	T_e	750, 1500, 2500	3
			N_e	10^{19}, 10^{20}, 10^{21}, 10^{22}, 10^{23}, 10^{24}	6

If the upper limit used in autoionization is 10^{14} s^{-1} at high temperatures the values in Table 6 are obtained. Greater values more centered in the range of codes for higher temperatures can be computed with other formulas with upper limit of the order of magnitude 10^{17} s^{-1} [22,23].

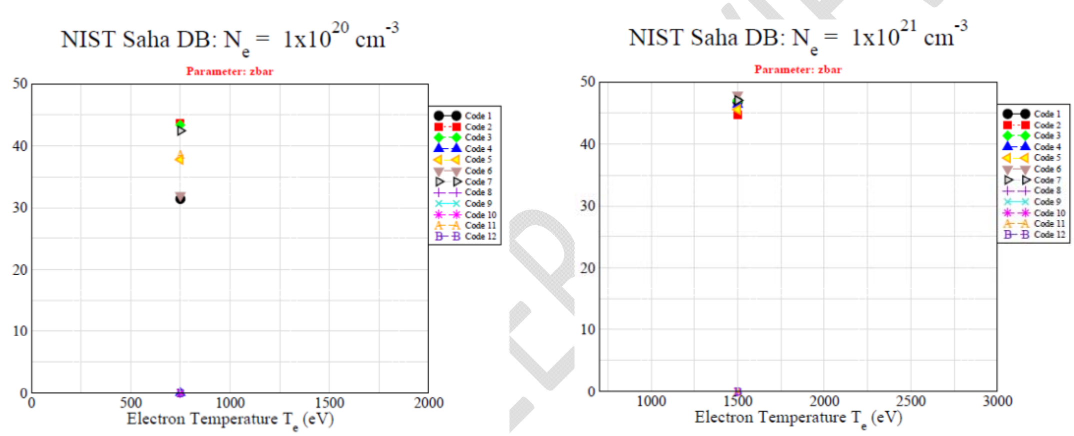

Figure 6.a. Gold plasma properties computed with codes of NLTE-3 Workshop

Table 6.a. Gold plasma properties of ATMED CR for comparison with codes of NLTE-3 Workshop

N_e (cm^{-3}) = 10^{19}	ρ (g/cm^3)	Z_{bar} ATMED	Z_{bar} NLTE-3	η_e ATMED CR	RPL (1e-7 $J/cm^3/s$)
T_e = 750 eV	1.260E-04	2.670E+01	27÷43	-1.6305E+01	4.261264E+19
T_e = 1500 eV	9.154E-05	3.573E+01	39÷46	-1.7373E+01	3.316573E+19
T_e = 2500 eV	7.418E-05	4.409E+01	44÷50	-1.8139E+01	2.809442E+19
N_e (cm^{-3}) = 10^{20}	**ρ (g/cm^3)**	**Z_{bar} ATMED**	**Z_{bar} NLTE-3**	**η_e ATMED CR**	**RPL (1e-7 $J/cm^3/s$)**
T_e = 750 eV	1.100E-03	3.074E+01	30÷45	-1.3997E+01	8.934351E+20
T_e = 1500 eV	8.420E-04	3.890E+01	40÷47	-1.5069E+01	1.838753E+21
T_e = 2500 eV	7.200E-04	4.564E+01	45÷50	-1.5832E+01	2.339277E+21
N_e (cm^{-3}) = 10^{21}	**ρ (g/cm^3)**	**Z_{bar} ATMED**	**Z_{bar} NLTE-3**	**η_e ATMED CR**	**RPL (1e-7 $J/cm^3/s$)**
T_e = 750 eV	9.026E-03	3.625E+01	34÷45	-1.1728E+01	5.307210E+22
T_e = 1500 eV	7.540E-03	4.345E+01	44÷50	-1.2766E+01	8.309760E+22
T_e = 2500 eV	6.950E-03	4.718E+01	47÷50	-1.3532E+01	7.744388E+22

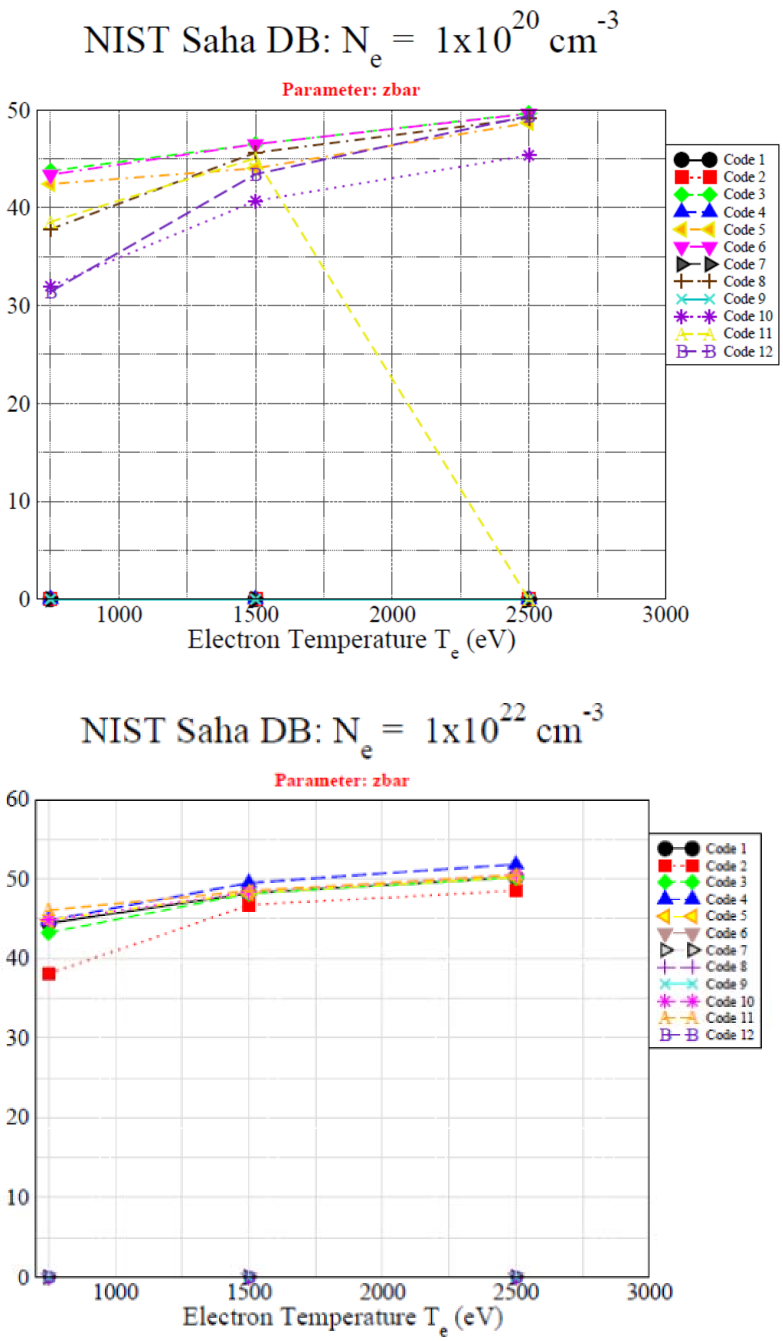

Figure 6.b. Gold plasma properties computed with codes of NLTE-3 Workshop

Table 6.b. Gold plasma properties of ATMED CR for comparison with codes of NLTE-3 Workshop

N_e (cm^{-3}) = 10^{22}	ρ (g/cm^3)	Z_{bar} ATMED	Z_{bar} NLTE-3	η_e ATMED CR	RPL (1e-7 J/cm^3/s)
T_e = 750 eV	7.884E-02	4.149E+01	37÷48	-9.4252E+00	1.211432E+24
T_e = 1500 eV	7.143E-02	4.579E+01	45÷51	-1.0465E+01	2.032188E+24
T_e = 2500 eV	6.748E-02	4.847E+01	46÷54	-1.1231E+01	1.100801E+24

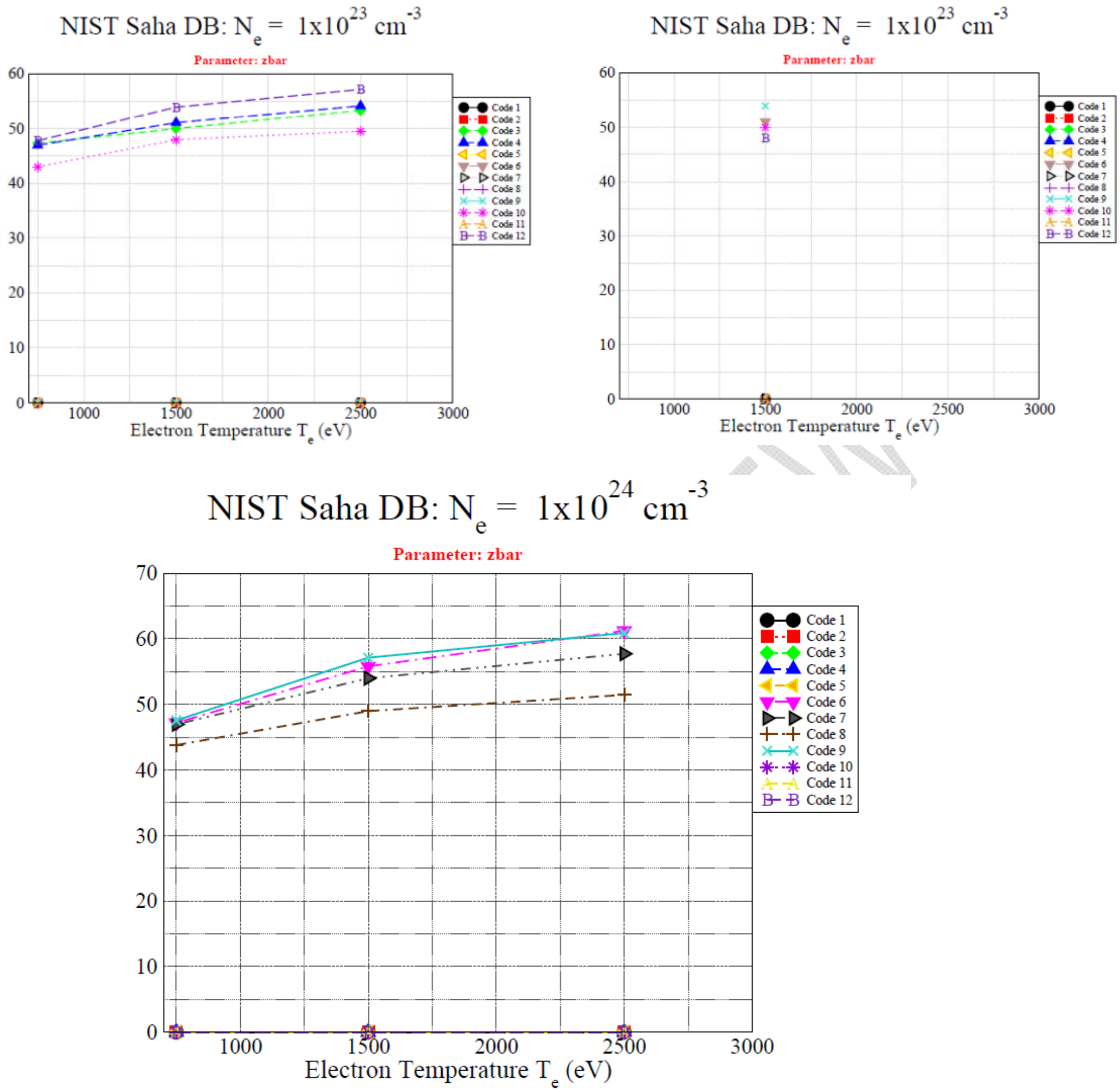

Figure 6.c. Gold plasma properties computed with codes of NLTE-3 Workshop

Table 6.c. Gold plasma properties of ATMED CR for comparison with codes of NLTE-3 Workshop

N_e (cm^{-3}) = 10^{23}	ρ (g/cm^3)	Z_{bar} ATMED	Z_{bar} NLTE-3	η_e ATMED CR	RPL (1e-7 J/cm^3/s)
T_e = 750 eV	7.549E-01	4.334E+01	42÷50	-7.1223E+00	1.127530E+27
T_e = 1500 eV	6.899E-01	4.741E+01	47÷55	-8.1624E+00	4.921110E+25
T_e = 2500 eV	6.501E-01	5.031E+01	49÷59	-8.9288E+00	4.974738E+25
N_e (cm^{-3}) = 10^{24}	ρ (g/cm^3)	Z_{bar} ATMED	Z_{bar} NLTE-3	η_e ATMED CR	RPL (1e-7 J/cm^3/s)
T_e = 750 eV	7.806E+00	4.193E+01	43÷49	-4.8167E+00	4.216810E+27
T_e = 1500 eV	6.682E+00	4.896E+01	48÷58	-5.8588E+00	2.782662E+28
T_e = 2500 eV	6.060E+00	5.427E+01	50÷62	-6.6203E+00	4.795663E+27

2.6 Germanium Time Dependent Plasma

The following problem has been established for the temporal case of germanium X-ray laser plasma, see Table 7 and Figure 7. In Appendix I it is shown the time history of T_e (left hand axis) and N_e (right hand axis) for the TD-Ge case, which is motivated by the germanium X-ray laser experiments.

This calculation should be carried out to t = 1.975 ns, and the exigent non-uniform time grid along with the corresponding values of T_e and N_e are presented in Appendix I. The initial condition is LTE. In order not to entering in an infinite iterative loop or interrupted execution of FORTRAN code, the following criteria have been used for calculation with ATMED CR, considering matter density as the fundamental parameter for computation:

- There is a first loop of convergence in electronic density with criteria 1E-003, for coincidence up to the second decimal figure at least, with input parameter the N_e of the provided grid.
- There is a second loop inside the previous one of convergence in populations of electronic relativistic orbitals with criteria 1E-002.
- The computation with code ATMED CR starts at step 14 with conditions:

Step #	Time (s)	Te	Ne
14	5.3137E-10	2.0025E+02	2.4230E+20

- The computation with code ATMED CR ends at step 82 with conditions:

Step #	Time (s)	Te	Ne
82	1.9749E-09	3.4240E+02	1.2526E+20

Some results are displayed in Appendix I, Figure 7 and Table 7, being the acronyms as follows:

- **BB, BF, FF and Total RPL** Bound-Bound, Bound-Free, Free-Free and Total Radiative Power Losses in J/(cm^3.s).
- **$<S_{tot}>$** The total ionization rate out of the average atom. This quantity is further summed over all ionization processes.
- **$<f\_S_{coll}>$** The fractional contribution of electron collisional ionization processes to **$<S_{tot}>$.**
- **$<f\_S_{photo}>$** The fractional contribution of photo-ionization processes to **$<S_{tot}>$.**
- **$<f\_S_{auto}>$** The fractional contribution of auto-ionization processes to **$<S_{tot}>$**.

- $\langle \alpha_{tot} \rangle$ The total recombination rate of the average atom. This quantity is further summed over all recombination processes.
- $\langle f\_\alpha_{coll} \rangle$ The fractional contribution of three-body recombination to the total $\langle \alpha_{tot} \rangle$.
- $\langle f\_\alpha_{photo} \rangle$ The fractional contribution of radiative-recombination to the total $\langle \alpha_{tot} \rangle$.
- $\langle f\_\alpha_{auto} \rangle$ The fractional contribution of dielectronic capture processes to the total $\langle \alpha_{tot} \rangle$.
- $\langle \Gamma_{tot} \rangle$ The total population flux out of the average atom. Units are s^{-1}.
- $\langle f\_\Gamma_{collBB} \rangle$ The fractional contribution of electron collision excitation/de-excitation processes to $\langle \Gamma_{tot} \rangle$.
- $\langle f\_\Gamma_{photoBB} \rangle$ The fractional contribution of bound-bound radiation processes to $\langle \Gamma_{tot} \rangle$.
- $\langle f\_\Gamma_{collBF} \rangle$ The fractional contribution of electron collision ionization-recombination processes to $\langle \Gamma_{tot} \rangle$.
- $\langle f\_\Gamma_{photoBF} \rangle$ The fractional contribution of photo-ionization-recombination to $\langle \Gamma_{tot} \rangle$.
- $\langle f\_\Gamma_{auto} \rangle$ The fractional contribution of auto-ionization/dielectronic recombination processes to $\langle \Gamma_{tot} \rangle$.
- $\langle \Theta_{tot} \rangle$ The total population flux into the average atom. Units are s^{-1}.
- $\langle f\_\Theta_{collBB} \rangle$ The fractional contribution of electron collision excitation/de-excitation processes to $\langle \Theta_{tot} \rangle$.
- $\langle f\_\Theta_{photoBB} \rangle$ The fractional contribution of bound-bound radiation processes to $\langle \Theta_{tot} \rangle$.
- $\langle f\_\Theta_{collBF} \rangle$ The fractional contribution of electron collision ionization-recombination processes to $\langle \Theta_{tot} \rangle$.
- $\langle f\_\Theta_{photoBF} \rangle$ The fractional contribution of photo-ionization-recombination to $\langle \Theta_{tot} \rangle$.
- $\langle f\_\Theta_{auto} \rangle$ The fractional contribution of auto-ionization/dielectronic recombination processes to $\langle \Theta_{tot} \rangle$.
- **<occ1>** Fractional occupation number of electrons in the K shell of the average atom.
- **<occ2>** The fractional number of electrons in the L shell of the average atom.

…

Table 7.a. Ge plasma properties of ATMED CR for 4 temporal representative intervals

Step	Time (s)	BB RPL	BF RPL	FF RPL	Total RPL
14	**5.313700E-10**	1.869183E+11	4.870430E+05	8.036349E+07	1.869991E+11
36	**8.657700E-10**	1.600383E+10	1.458753E+05	4.774089E+07	1.605172E+10
58	**1.084400E-09**	4.094735E+09	1.116198E+05	3.547699E+07	4.130324E+09
82	**1.974900E-09**	8.684380E+07	1.870771E+05	2.155397E+07	1.085848E+08
Step	**Time (s)**	**<S_{tot}>**	**<f_S_{coll}>**	**<f_S_{photo}>**	**<f_S_{auto}>**
14	**5.313700E-10**	1.014657E+16	8.384767E-05	0.000000E+00	9.999162E-01
36	**8.657700E-10**	9.931239E+14	8.173540E-04	0.000000E+00	9.991826E-01
58	**1.084400E-09**	8.198916E+14	8.470501E-04	0.000000E+00	9.991529E-01
82	**1.974900E-09**	3.044400E+13	6.215985E-03	0.000000E+00	9.937840E-01
Step	**Time (s)**	**<α_{tot}>**	**<f_α_{coll}>**	**<f_α_{photo}>**	**<f_α_{auto}>**
14	**5.313700E-10**	2.364472E+12	1.674265E-05	0.000000E+00	9.999833E-01
36	**8.657700E-10**	1.805011E+10	8.095559E-05	0.000000E+00	9.999190E-01
58	**1.084400E-09**	5.991476E+09	1.762400E-04	0.000000E+00	9.998238E-01
82	**1.974900E-09**	1.417566E+07	1.470520E-01	0.000000E+00	8.529480E-01

Table 7.b. Ge plasma properties of ATMED CR for 4 temporal representative intervals

Time (s)	<Γ_{tot}>	<f_Γ_{collBB}>	<f_$\Gamma_{photoBB}$>	<f_Γ_{collBF}>	<f_$\Gamma_{photoBF}$>	<f_Γ_{auto}>
5.313700E-10	1.345911E+16	2.452333E-01	0.000000E+00	6.321120E-05	0.000000E+00	7.547035E-01
8.657700E-10	2.325453E+15	5.714696E-01	0.000000E+00	3.490649E-04	0.000000E+00	4.281813E-01
1.084400E-09	1.974015E+15	5.831757E-01	0.000000E+00	3.518155E-04	0.000000E+00	4.164724E-01
1.974900E-09	1.203081E+15	9.720865E-01	0.000000E+00	1.572956E-04	0.000000E+00	2.775621E-02
Time (s)	**<Θ_{tot}>**	**<f_Θ_{collBB}>**	**<f_$\Theta_{photoBB}$>**	**<f_Θ_{collBF}>**	**<f_$\Theta_{photoBF}$>**	**<f_Θ_{auto}>**
5.313700E-10	1.214971E+18	5.176583E-06	0.000000E+00	3.258312E-11	0.000000E+00	9.999948E-01
8.657700E-10	2.805846E+12	1.088537E-02	0.000000E+00	5.207904E-07	0.000000E+00	9.891141E-01
1.084400E-09	6.179158E+10	1.171259E-01	0.000000E+00	1.708870E-05	0.000000E+00	8.828570E-01
1.974900E-09	6.572407E+08	8.989837E-01	0.000000E+00	3.171684E-03	0.000000E+00	9.784461E-02
Time (s)	**<occ1>**	**<occ2>**	**<occ3>**	**<occ4>**	**<occ5>**	**<occ6>**
5.313700E-10	1.996457	7.135317	0.043153	0.007621	0.002039	0.000068
8.657700E-10	1.994999	0.014036	0.000737	0.000538	0.000236	0.000012
1.084400E-09	1.900191	0.001187	0.000206	0.000182	0.000083	0.000004
1.974900E-09	1.892914	0.000016	0.000015	0.000016	0.000008	0.000000

In Appendix I it is shown the whole time history of mean charge, matter and ionic density and relativistic orbital populations in the average atom for all temporal intervals, being the depletion of L-shell extremely rapid (<occ2>). In Table 2 it is also displayed the electronic density after computation used by ATMED CR versus the input value of N_e.

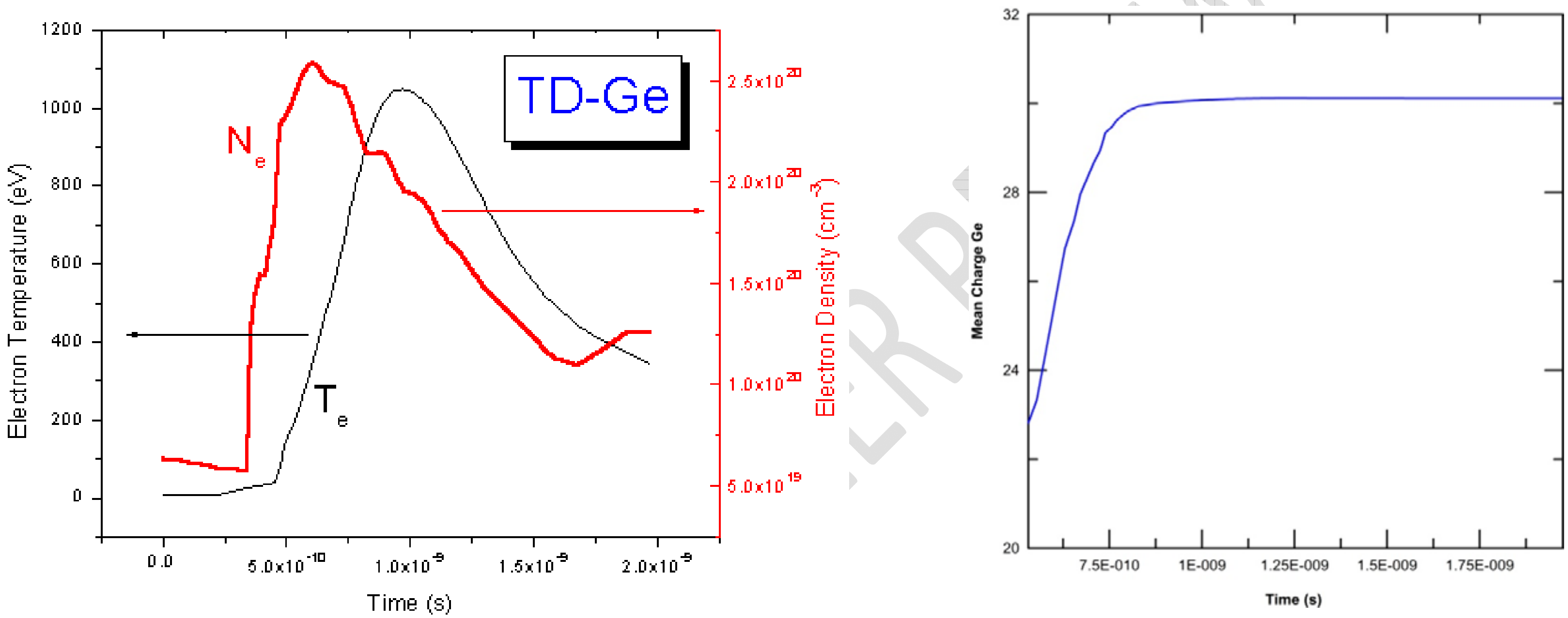

Figure 7.a. Time history of plasma parameters for TD-Ge provided by Workshop NLTE-3 (left). Temporal mean charge of germanium plasma computed with ATMED CR (right).

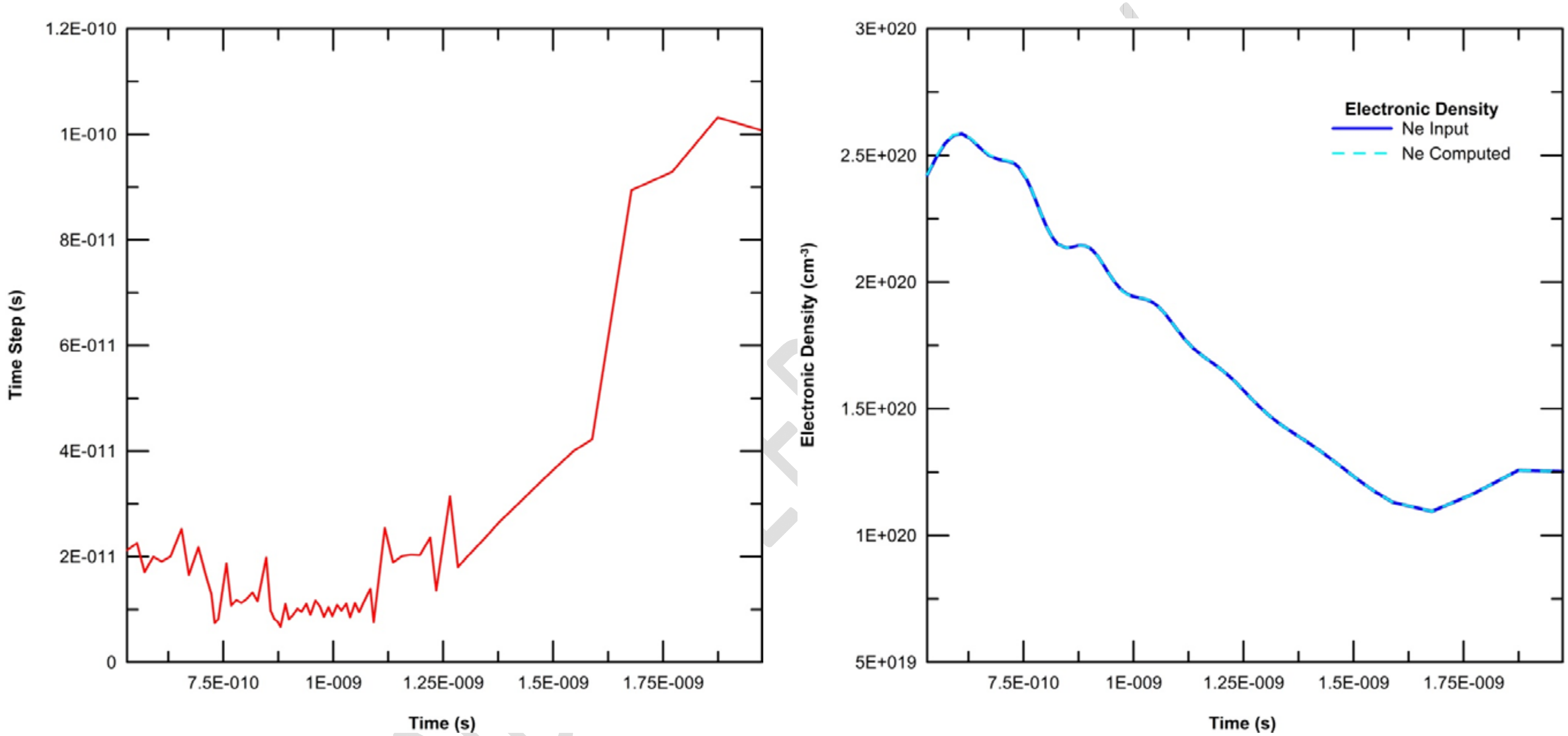

Figure 7.b. Time step evolution of plasma case TD-Ge provided by Workshop NLTE-3 (left). Profiles used by ATMED CR: electronic temperature as input parameter and computed electronic density with criteria of convergence 1E-002 for matching each value of electronic density as input parameter at the belonging temporal interval (right).

3. SUMMARY AND CONCLUSIONS

In this paper, there are modeled with ATMED CR plasmas proposed in the 3rd Non-LTE Code Comparison Workshop held in December 2003. Cases for C, Al, Ar, Ge, Xe and Au plasmas were selected for detailed comparisons. It has been observed a good agreement of atomic and radiative properties with respect to results of other codes which have participated in the storage inside the 3rd NLTE database [18-19]. A very complete description of the code ATMED CR can be found in both books of the doctoral thesis [2,24].

References

[1] A.J. Benita, E. Mínguez, M.A. Mendoza, J.G. Rubiano, J.M. Gil, R. Rodríguez, P. Martel. Collisional Radiative Average Atom Code Based on a Relativistic Screened Hydrogenic Model. High Energy Density Physics 14 (2015) 18-29.

[2] A.J. Benita. Collisional Radiative Average Atom Code With Relativistic Atomic Model. Theoretical physics. ISBN: 978-620-2-01943-9. LAP Lambert Academic Publishing (2017).

[3] A.J. Benita. Fast Calculation of Plasmas Properties with ATMED LTE. Project of Nuclear Science and Technology Master at UPM (2012).

[4] M.A. Mendoza, J.G. Rubiano, J.M. Gil, R. Rodriguez, R. Florido, A.J. Benita, P. Martel, E. Minguez. Fast Computation of Radiative Properties and EOS of Warm Dense Matter using the ATMED code. Eight International Conference on Inertial Fusion Sciences and Applications (IFSA 2013). September 8 -13 (2013) Nara, Japan.

[5] M.A. Mendoza, J.G. Rubiano, J.M. Gil, R. Rodriguez, R. Florido, G. Espinosa, P. Martel, E. Minguez. Calculation of radiative opacity of plasma mixtures using a relativistic screened hydrogenic model. Journal of Quantitative Spectroscopy & Radiative Transfer 140 (2014) 81–98.

[6] M.A. Mendoza, J.G. Rubiano, J.M. Gil, R. Rodriguez, R. Florido, P. Martel, E. Minguez. A new set of relativistic screening constants for the screened hydrogenic model. HEDP 7 (2011) 169–179.

[7] F.H. Ruano, J.G. Rubiano, M.A. Mendoza, J.M.Gil, R. Rodriguez, R. Florido, P. Martel, E. Minguez. Relativistic screened hydrogenic radial integrals. Journal of Quantitative Spectroscopy & Radiative Transfer (2012) 117123-132.

[8] W.A. Lokke and W.H. Grasberger. XSNQ-U A Non-LTE Emission and Absorption Coefficient Subroutine. Prepared for U.S. Energy Research & Development Administration under contract No. W-7405-Eng-48, UCRL-52276 (1977).

[9] Joseph Abdallah et al. The reduced detailed configuration accounting (RDCA) model for NLTE plasma calculations. High Energy Density Physics 4 (2008) 124–130.

[10] G.Faussurier, C. Blancard, T. Kato, R. M. More. Prigogine theorem of minimum entropy production applied to the average atom model. High Energy Density Physics 5 (2009) 283–293.

[11] G.Faussurier et al. Nonlocal thermodynamic equilibrium self-consistent average-atom model for plasma physics. PHYSICAL REVIEW E, VOLUME 63, 026401 (2001).

[12] Balazs F. Rozsnyai. Collisional radiative average atom model for hot plasmas. Physical Review E 55, (1996).

[13] Balazs F. Rozsnyai. Hot plasma opacities in the presence or absence of local thermodynamic equilibrium. High Energy Density Physics 6 (2010) 345–355.

[14] A.F. Nikiforov, V.G. Novikov, V.B. Uvarov. Quantum-statistical models of hot dense matter. Methods for Computation Opacity and Equation of State. Birkhäuser Verlag (2005).

[15] A.J. Benita. Calculation of Temporal Plasmas of XFEL Experiments with a Relativistic Collisional Radiative Average Atom Code. Physical Science International Journal, DOI: 10.9734/PSIJ/2018/40246 (2018).

[16] A.J. Benita. Book Summary ISBN 978-620-2-01943-9. https://www.researchgate.net/profile/Aj_Benita (2017).

[17] A.J. Benita. Comparison of Iron Plasma Atomic and Radiative Properties Computed with a Relativistic Collisional Radiative Average Atom Code versus Other Models. Asian Journal of Research and Reviews in Physics, DOI: 10.9734/AJR2P/2018/41729 (2018).

[18] https://nlte.nist.gov/SAHA/

[19] The Third Non-LTE Kinetics Workshop. Submission of Calculations. December 1-5, 2003. NIST, Gaithersburg MD.

[20] Plasmas Computed with ATMED CR of the 4th Non-LTE Code Comparison Workshop Database. Physical Science International Journal 20(1): 1-26, 2018; Article no.PSIJ.44683, ISSN: 2348-0130, DOI: 10.9734/PSIJ/2018/44683.

[21] R. Florido et al. Modeling of population kinetics of plasmas that are not in local thermodynamic equilibrium, using a versatile collisional-radiative model based on analytical rates. PHYSICAL REVIEW E 80, 056402 (2009), DOI: 10.1103/PhysRevE.80.056402.

[22] H.-K. Chung et al. FLYCHK : Generalized population kinetics and spectral model for rapid spectroscopic analysis for all elements. UCRL-JRNL-213347. High Energy Density Physics (2005).

[23] H.A. Scott and S.B. Hansen. Advances in NLTE modeling for integrated simulations. High Energy Density Physics 6 (2010) 39–47.

[24] Benita AJ. Set of Plasmas with Relativistic Collisional Radiative Code ATMED CR. Physics, astronomy. ISBN: 978-613-9-94744-7. LAP Lambert Academic Publishing; 2019.

4. APPENDIX I

Table 1. Evolution of germanium plasma parameters depending on the characteristics of the experiment with ATMED CR and considering plasma effects with ionization pressure (IP) similar to Ecker-Kröll model.

Time (s)	T_e (eV)	N_e (cm^{-3})	ρ g/cm^3	Mean Charge Z_{bar}	N_{ion} ($ion.cm^{-3}$)	Time Step (s)
5.313700E-10	**200.250000**	2.424698E+20	0.001282	22.815345	1.062749E+19	2.123000E-11
5.539300E-10	**241.300000**	2.500567E+20	0.001293	23.326896	1.071967E+19	2.256000E-11
5.710200E-10	**274.370000**	2.546749E+20	0.001276	24.083975	1.057446E+19	1.709000E-11
5.910000E-10	**316.800000**	2.580686E+20	0.001246	24.976002	1.033266E+19	1.998000E-11
6.100800E-10	**359.320000**	2.586875E+20	0.001207	25.843447	1.000979E+19	1.908000E-11
6.301000E-10	**406.130000**	2.566818E+20	0.001158	26.735054	9.600946E+18	2.002000E-11
6.553400E-10	**467.340000**	2.526143E+20	0.001113	27.372312	9.228825E+18	2.524000E-11
6.718600E-10	**505.070000**	2.502619E+20	0.001079	27.966913	8.948499E+18	1.652000E-11
6.936300E-10	**560.720000**	2.485272E+20	0.001056	28.383184	8.756144E+18	2.177000E-11
7.101700E-10	**606.760000**	2.479839E+20	0.001042	28.708959	8.637856E+18	1.654000E-11
7.230600E-10	**642.860000**	2.474014E+20	0.001032	28.903661	8.559518E+18	1.289000E-11
7.304800E-10	**663.730000**	2.467273E+20	0.001023	29.085627	8.482790E+18	7.420000E-12
7.386500E-10	**686.850000**	2.456407E+20	0.001010	29.336979	8.373075E+18	8.170000E-12
7.573800E-10	**740.030000**	2.406867E+20	0.000985	29.477481	8.165105E+18	1.873000E-11
7.681100E-10	**770.070000**	2.365830E+20	0.000964	29.600173	7.992621E+18	1.073000E-11
7.799100E-10	**802.460000**	2.314356E+20	0.000940	29.695725	7.793567E+18	1.180000E-11
7.911600E-10	**831.520000**	2.264476E+20	0.000917	29.774609	7.605392E+18	1.125000E-11
8.031600E-10	**861.980000**	2.215932E+20	0.000896	29.839629	7.426139E+18	1.200000E-11
8.163500E-10	**894.560000**	2.174250E+20	0.000878	29.886725	7.274968E+18	1.319000E-11
8.279100E-10	**919.150000**	2.150185E+20	0.000866	29.938795	7.181936E+18	1.156000E-11
8.477300E-10	**955.330000**	2.135551E+20	0.000860	29.962001	7.127530E+18	1.982000E-11
8.575400E-10	**971.750000**	2.137331E+20	0.000860	29.977996	7.129666E+18	9.810000E-12
8.657700E-10	**983.600000**	2.140821E+20	0.000861	29.989442	7.138584E+18	8.230000E-12
8.734400E-10	**993.690000**	2.144019E+20	0.000862	29.997001	7.147445E+18	7.670000E-12
8.801600E-10	**1001.700000**	2.145422E+20	0.000862	30.005788	7.150027E+18	6.720000E-12
8.911800E-10	**1013.200000**	2.143024E+20	0.000861	30.011562	7.140660E+18	1.102000E-11
8.993200E-10	**1020.600000**	2.136324E+20	0.000858	30.017511	7.116925E+18	8.140000E-12
9.082000E-10	**1027.400000**	2.123628E+20	0.000853	30.023931	7.073117E+18	8.880000E-12
9.183600E-10	**1033.900000**	2.102835E+20	0.000845	30.029715	7.002515E+18	1.016000E-11
9.279400E-10	**1038.700000**	2.078639E+20	0.000835	30.036117	6.920465E+18	9.580000E-12
9.390000E-10	**1043.100000**	2.048024E+20	0.000822	30.041364	6.817348E+18	1.106000E-11
9.479800E-10	**1045.500000**	2.023524E+20	0.000812	30.047902	6.734328E+18	8.980000E-12
9.596900E-10	**1047.100000**	1.994821E+20	0.000801	30.053532	6.637559E+18	1.171000E-11
9.701800E-10	**1047.200000**	1.972206E+20	0.000791	30.057847	6.561369E+18	1.049000E-11
9.787600E-10	**1046.500000**	1.959588E+20	0.000786	30.062807	6.518313E+18	8.580000E-12

9.892000E-10	**1045.300000**	1.948918E+20	0.000782	30.066872	6.481944E+18	1.044000E-11
9.979500E-10	**1043.300000**	1.943491E+20	0.000780	30.071552	6.462889E+18	8.750000E-12
1.008800E-09	**1039.900000**	1.939413E+20	0.000778	30.075616	6.448456E+18	1.085000E-11
1.018600E-09	**1035.700000**	1.936582E+20	0.000777	30.079900	6.438128E+18	9.800000E-12
1.029700E-09	**1030.200000**	1.932111E+20	0.000775	30.082981	6.422605E+18	1.110000E-11
1.038200E-09	**1025.800000**	1.926560E+20	0.000772	30.086685	6.403363E+18	8.500000E-12
1.049400E-09	**1019.700000**	1.914993E+20	0.000768	30.089606	6.364301E+18	1.120000E-11
1.058900E-09	**1014.000000**	1.899002E+20	0.000761	30.092921	6.310461E+18	9.500000E-12
1.070500E-09	**1006.300000**	1.877404E+20	0.000752	30.096437	6.237960E+18	1.160000E-11
1.084400E-09	**996.040000**	1.846700E+20	0.000740	30.098146	6.135595E+18	1.390000E-11
1.092000E-09	**989.940000**	1.829106E+20	0.000733	30.103068	6.076146E+18	7.600000E-12
1.117400E-09	**967.750000**	1.772702E+20	0.000710	30.105789	5.888242E+18	2.540000E-11
1.136300E-09	**949.800000**	1.738600E+20	0.000697	30.107968	5.774553E+18	1.890000E-11
1.156400E-09	**928.870000**	1.709800E+20	0.000685	30.109533	5.678601E+18	2.010000E-11
1.176800E-09	**906.070000**	1.684700E+20	0.000675	30.110548	5.595050E+18	2.040000E-11
1.197100E-09	**881.970000**	1.659100E+20	0.000665	30.111219	5.509906E+18	2.030000E-11
1.220700E-09	**853.820000**	1.624200E+20	0.000651	30.111403	5.393970E+18	2.360000E-11
1.234300E-09	**837.200000**	1.601300E+20	0.000641	30.111473	5.317908E+18	1.360000E-11
1.265700E-09	**799.130000**	1.544300E+20	0.000619	30.111384	5.128626E+18	3.140000E-11
1.283700E-09	**776.940000**	1.512300E+20	0.000606	30.111195	5.022385E+18	1.800000E-11
1.303600E-09	**752.750000**	1.480300E+20	0.000593	30.110953	4.916151E+18	1.990000E-11
1.325400E-09	**726.670000**	1.449600E+20	0.000581	30.110677	4.814240E+18	2.180000E-11
1.349300E-09	**698.780000**	1.420300E+20	0.000569	30.110394	4.716976E+18	2.390000E-11
1.375700E-09	**669.690000**	1.390600E+20	0.000557	30.110122	4.618381E+18	2.640000E-11
1.404400E-09	**639.490000**	1.357800E+20	0.000544	30.109875	4.509484E+18	2.870000E-11
1.435600E-09	**608.890000**	1.319400E+20	0.000529	30.109652	4.381984E+18	3.120000E-11
1.469600E-09	**578.210000**	1.274500E+20	0.000511	30.109458	4.232890E+18	3.400000E-11
1.506500E-09	**548.070000**	1.225000E+20	0.000491	30.109282	4.068513E+18	3.690000E-11
1.546500E-09	**518.510000**	1.175400E+20	0.000471	30.109122	3.903801E+18	4.000000E-11
1.588700E-09	**492.100000**	1.131400E+20	0.000453	30.108805	3.757706E+18	4.220000E-11
1.678100E-09	**442.950000**	1.095200E+20	0.000439	30.108488	3.637514E+18	8.940000E-11
1.771000E-09	**403.690000**	1.163200E+20	0.000466	30.108065	3.863418E+18	9.290000E-11
1.874200E-09	**369.570000**	1.256901E+20	0.000504	30.107543	4.174704E+18	1.032000E-10
1.974900E-09	**342.400000**	1.252603E+20	0.000502	30.107030	4.160501E+18	1.007000E-10

Table 2. Data for comparison of input density with the density ATMED CR computes for the iterative loop checking the coincidence up to the second decimal figure at least followed by power E+20.

Step #	Time (s)	T_e	N_e	ATMED CR N_e
14	5.3137E-10	2.0025E+02	**2.4230E+20**	2.424698E+20
15	5.5393E-10	2.4130E+02	**2.4981E+20**	2.500567E+20
16	5.7102E-10	2.7437E+02	**2.5455E+20**	2.546749E+20
17	5.9100E-10	3.1680E+02	**2.5793E+20**	2.580686E+20
18	6.1008E-10	3.5932E+02	**2.5855E+20**	2.586875E+20
19	6.3010E-10	4.0613E+02	**2.5655E+20**	2.566818E+20
20	6.5534E-10	4.6734E+02	**2.5237E+20**	2.526143E+20
21	6.7186E-10	5.0507E+02	**2.5003E+20**	2.502619E+20
22	6.9363E-10	5.6072E+02	**2.4833E+20**	2.485272E+20
23	7.1017E-10	6.0676E+02	**2.4784E+20**	2.479839E+20
24	7.2306E-10	6.4286E+02	**2.4730E+20**	2.474014E+20
25	7.3048E-10	6.6373E+02	**2.4664E+20**	2.467273E+20
26	7.3865E-10	6.8685E+02	**2.4546E+20**	2.456407E+20
27	7.5738E-10	7.4003E+02	**2.4056E+20**	2.406867E+20
28	7.6811E-10	7.7007E+02	**2.3649E+20**	2.365830E+20
29	7.7991E-10	8.0246E+02	**2.3137E+20**	2.314356E+20
30	7.9116E-10	8.3152E+02	**2.2640E+20**	2.264476E+20
31	8.0316E-10	8.6198E+02	**2.2157E+20**	2.215932E+20
32	8.1635E-10	8.9456E+02	**2.1741E+20**	2.174250E+20
33	8.2791E-10	9.1915E+02	**2.1501E+20**	2.150185E+20
34	8.4773E-10	9.5533E+02	**2.1355E+20**	2.135551E+20
35	8.5754E-10	9.7175E+02	**2.1373E+20**	2.137331E+20
36	8.6577E-10	9.8360E+02	**2.1408E+20**	2.140821E+20
37	8.7344E-10	9.9369E+02	**2.1440E+20**	2.144019E+20
38	8.8016E-10	1.0017E+03	**2.1454E+20**	2.145422E+20
39	8.9118E-10	1.0132E+03	**2.1430E+20**	2.143024E+20
40	8.9932E-10	1.0206E+03	**2.1363E+20**	2.136324E+20
41	9.0820E-10	1.0274E+03	**2.1236E+20**	2.123628E+20
42	9.1836E-10	1.0339E+03	**2.1028E+20**	2.102835E+20
43	9.2794E-10	1.0387E+03	**2.0786E+20**	2.078639E+20
44	9.3900E-10	1.0431E+03	**2.0480E+20**	2.048024E+20
45	9.4798E-10	1.0455E+03	**2.0235E+20**	2.023524E+20
46	9.5969E-10	1.0471E+03	**1.9948E+20**	1.994821E+20
47	9.7018E-10	1.0472E+03	**1.9739E+20**	1.972206E+20
48	9.7876E-10	1.0465E+03	**1.9610E+20**	1.959588E+20
49	9.8920E-10	1.0453E+03	**1.9500E+20**	1.948918E+20
50	9.9795E-10	1.0433E+03	**1.9442E+20**	1.943491E+20

Table 2. Data for comparison of input density with the density ATMED CR computes for the iterative loop checking the coincidence up to the second decimal figure at least followed by power E+20.

Step #	Time (s)	T_e	N_e	ATMED CR N_e
51	1.0088E-09	1.0399E+03	**1.9396E+20**	1.939413E+20
52	1.0186E-09	1.0357E+03	**1.9363E+20**	1.936582E+20
53	1.0297E-09	1.0302E+03	**1.9313E+20**	1.932111E+20
54	1.0382E-09	1.0258E+03	**1.9253E+20**	1.926560E+20
55	1.0494E-09	1.0197E+03	**1.9132E+20**	1.914993E+20
56	1.0589E-09	1.0140E+03	**1.8990E+20**	1.899002E+20
57	1.0705E-09	1.0063E+03	**1.8774E+20**	1.877404E+20
58	1.0844E-09	9.9604E+02	**1.8467E+20**	1.846700E+20
59	1.0920E-09	9.8994E+02	**1.8291E+20**	1.829106E+20
60	1.1174E-09	9.6775E+02	**1.7727E+20**	1.772702E+20
61	1.1363E-09	9.4980E+02	**1.7386E+20**	1.738600E+20
62	1.1564E-09	9.2887E+02	**1.7098E+20**	1.709800E+20
63	1.1768E-09	9.0607E+02	**1.6847E+20**	1.684700E+20
64	1.1971E-09	8.8197E+02	**1.6591E+20**	1.659100E+20
65	1.2207E-09	8.5382E+02	**1.6242E+20**	1.624200E+20
66	1.2343E-09	8.3720E+02	**1.6013E+20**	1.601300E+20
67	1.2657E-09	7.9913E+02	**1.5443E+20**	1.544300E+20
68	1.2837E-09	7.7694E+02	**1.5123E+20**	1.512300E+20
69	1.3036E-09	7.5275E+02	**1.4803E+20**	1.480300E+20
70	1.3254E-09	7.2667E+02	**1.4496E+20**	1.449600E+20
71	1.3493E-09	6.9878E+02	**1.4203E+20**	1.420300E+20
72	1.3757E-09	6.6969E+02	**1.3906E+20**	1.390600E+20
73	1.4044E-09	6.3949E+02	**1.3578E+20**	1.357800E+20
74	1.4356E-09	6.0889E+02	**1.3194E+20**	1.319400E+20
75	1.4696E-09	5.7821E+02	**1.2745E+20**	1.274500E+20
76	1.5065E-09	5.4807E+02	**1.2250E+20**	1.225000E+20
77	1.5465E-09	5.1851E+02	**1.1754E+20**	1.175400E+20
78	1.5887E-09	4.9210E+02	**1.1314E+20**	1.131400E+20
79	1.6781E-09	4.4295E+02	**1.0952E+20**	1.095200E+20
80	1.7710E-09	4.0369E+02	**1.1632E+20**	1.163200E+20
81	1.8742E-09	3.6957E+02	**1.2569E+20**	1.256901E+20
82	1.9749E-09	3.4240E+02	**1.2526E+20**	1.252603E+20

Table 3. Evolution of germanium plasma fractional orbital populations in the average atom computed with ATMED CR.

Time (s)	<occ1>	<occ2>	<occ3>	<occ4>	<occ5>	<occ6>
5.313700E-10	1.996457	7.135317	0.043153	0.007621	0.002039	0.000068
5.539300E-10	1.996447	6.626846	0.038425	0.008803	0.002494	0.000089
5.710200E-10	1.996463	5.876843	0.031700	0.008434	0.002494	0.000092
5.910000E-10	1.996490	4.989918	0.026538	0.008461	0.002495	0.000095
6.100800E-10	1.996527	4.127288	0.022358	0.007858	0.002427	0.000095
6.301000E-10	1.996575	3.240534	0.018425	0.007053	0.002269	0.000091
6.553400E-10	1.996619	2.606513	0.015616	0.006603	0.002244	0.000094
6.718600E-10	1.996654	2.015504	0.013059	0.005778	0.002007	0.000085
6.936300E-10	1.996678	1.601757	0.011137	0.005264	0.001898	0.000083
7.101700E-10	1.996693	1.278159	0.009606	0.004750	0.001756	0.000078
7.230600E-10	1.996703	1.084867	0.008632	0.004405	0.001658	0.000074
7.304800E-10	1.996713	0.904328	0.007732	0.004010	0.001522	0.000068
7.386500E-10	1.996727	0.655132	0.006416	0.003390	0.001296	0.000059
7.573800E-10	1.996754	0.516038	0.005478	0.003016	0.001178	0.000054
7.681100E-10	1.996777	0.394683	0.004662	0.002621	0.001036	0.000048
7.799100E-10	1.996803	0.300302	0.003950	0.002269	0.000908	0.000043
7.911600E-10	1.996827	0.222494	0.003308	0.001940	0.000784	0.000037
8.031600E-10	1.996848	0.158481	0.002717	0.001629	0.000665	0.000032
8.163500E-10	1.996856	0.112230	0.002228	0.001368	0.000565	0.000027
8.279100E-10	1.996811	0.061314	0.001610	0.001023	0.000426	0.000021
8.477300E-10	1.996645	0.038897	0.001254	0.000832	0.000353	0.000017
8.575400E-10	1.996203	0.023855	0.000970	0.000672	0.000289	0.000014
8.657700E-10	1.994999	0.014036	0.000737	0.000538	0.000236	0.000012
8.734400E-10	1.992706	0.009039	0.000588	0.000453	0.000202	0.000010
8.801600E-10	1.987522	0.005665	0.000465	0.000380	0.000172	0.000009
8.911800E-10	1.982887	0.004605	0.000420	0.000355	0.000163	0.000008
8.993200E-10	1.977705	0.003898	0.000388	0.000335	0.000154	0.000008
9.082000E-10	1.971848	0.003385	0.000363	0.000319	0.000148	0.000007
9.183600E-10	1.966425	0.003057	0.000345	0.000308	0.000143	0.000007
9.279400E-10	1.960348	0.002764	0.000329	0.000296	0.000138	0.000007
9.390000E-10	1.955316	0.002574	0.000317	0.000287	0.000134	0.000007
9.479800E-10	1.949017	0.002363	0.000304	0.000277	0.000129	0.000007
9.596900E-10	1.943569	0.002205	0.000293	0.000268	0.000125	0.000006
9.701800E-10	1.939388	0.002090	0.000284	0.000262	0.000123	0.000006
9.787600E-10	1.934563	0.001974	0.000276	0.000254	0.000119	0.000006
9.892000E-10	1.930604	0.001884	0.000270	0.000248	0.000116	0.000006
9.979500E-10	1.926035	0.001789	0.000263	0.000242	0.000113	0.000006
1.008800E-09	1.922074	0.001704	0.000256	0.000235	0.000110	0.000006
1.018600E-09	1.917894	0.001618	0.000249	0.000228	0.000106	0.000005

1.029700E-09	1.914902	0.001545	0.000243	0.000221	0.000103	0.000005
1.038200E-09	1.911285	0.001474	0.000237	0.000215	0.000100	0.000005
1.049400E-09	1.908450	0.001405	0.000230	0.000208	0.000096	0.000005
1.058900E-09	1.905221	0.001339	0.000223	0.000200	0.000092	0.000005
1.070500E-09	1.901804	0.001260	0.000215	0.000191	0.000088	0.000005
1.084400E-09	1.900191	0.001187	0.000206	0.000182	0.000083	0.000004
1.092000E-09	1.895360	0.001115	0.000198	0.000174	0.000080	0.000004
1.117400E-09	1.892814	0.000983	0.000182	0.000157	0.000071	0.000004
1.136300E-09	1.890763	0.000886	0.000170	0.000144	0.000065	0.000003
1.156400E-09	1.889328	0.000789	0.000157	0.000131	0.000059	0.000003
1.176800E-09	1.888440	0.000694	0.000145	0.000118	0.000053	0.000003
1.197100E-09	1.887890	0.000603	0.000133	0.000106	0.000047	0.000002
1.220700E-09	1.887835	0.000508	0.000120	0.000093	0.000040	0.000002
1.234300E-09	1.887837	0.000453	0.000112	0.000086	0.000037	0.000002
1.265700E-09	1.888071	0.000347	0.000095	0.000071	0.000030	0.000002
1.283700E-09	1.888336	0.000292	0.000086	0.000063	0.000027	0.000001
1.303600E-09	1.888651	0.000239	0.000076	0.000056	0.000024	0.000001
1.325400E-09	1.888996	0.000190	0.000067	0.000048	0.000021	0.000001
1.349300E-09	1.889343	0.000146	0.000057	0.000042	0.000018	0.000001
1.375700E-09	1.889671	0.000108	0.000048	0.000035	0.000015	0.000001
1.404400E-09	1.889966	0.000076	0.000039	0.000030	0.000013	0.000001
1.435600E-09	1.890227	0.000053	0.000032	0.000025	0.000011	0.000001
1.469600E-09	1.890449	0.000036	0.000025	0.000021	0.000010	0.000000
1.506500E-09	1.890646	0.000025	0.000020	0.000018	0.000009	0.000000
1.546500E-09	1.890819	0.000018	0.000017	0.000016	0.000008	0.000000
1.588700E-09	1.891144	0.000014	0.000015	0.000015	0.000007	0.000000
1.678100E-09	1.891465	0.000012	0.000013	0.000014	0.000007	0.000000
1.771000E-09	1.891885	0.000013	0.000014	0.000015	0.000007	0.000000
1.874200E-09	1.892402	0.000015	0.000015	0.000017	0.000008	0.000000
1.974900E-09	1.892914	0.000016	0.000015	0.000016	0.000008	0.000000